1
Characterization, Physical and Thermodynamic Properties of Oil Fractions

This chapter introduces the common methods for characterizing crude oils and petroleum fractions (i.e., oil fractions), and for estimating their thermophysical properties. We begin by defining the essential bulk and fractional properties for oil fractions, and by explaining the various types of distillation curves and their interconversion (Section 1.1). Next, we discuss the generation of pseudocomponents of oil fractions based on boiling-point ranges, and the estimation of density and molecular weight distributions of the resulting pseudocomponents (Section 1.2). Sections 1.3 to 1.6 present four hands-on workshops using Excel spreadsheets and Aspen HYSYS Petroleum Refining for the interconversion of distillation curve data, the extrapolation of an incomplete distillation-curve data, the calculation of the mean-average boiling point of a given oil fraction, and specifying the oil fraction in Aspen HYSYS Petroleum Refining. Section 1.7 introduces the essential thermophysical properties for developing refinery reaction and fractionation process models. Section 1.8 presents the useful methods for estimating the thermophysical properties (e.g., molecular weight, liquid density, critical properties, ideal gas heat capacity, and heat of vaporization) of pseudo-components of oil fractions. Section 1.9 describes the important thermodynamic models for refinery reaction and fractionation processes. Section 1.10 discusses the estimation methods for other physical properties such as flash point, freeze point and PNA (paraffin, naphthalene and aromatic) content of a refinery feed. Finally, Section 1.11 summarizes the conclusions of this chapter.

1.1
Crude Assay

Crude oils and petroleum fractions are the most important feedstocks for refining processes. To properly simulate the refining processes, we must have good understanding of the compositional information and thermophysical properties of crude oils and petroleum fractions. However, the complexity of molecular composition of crude oils and petroleum fractions makes it hardly possible to identity individual molecules. Instead, modern refiners use assay to characterize crude oils and petroleum fractions.

Table 1.1 A typical crude assay.

	Whole crude	C4 and C4 –	C5–74 °C	74–166 °C	166–480 °C	480–249 °C	249–537 °C	537 °C+
Cut volume, %	100	1.57	8.26	20.96	17.11	17.52	24.71	9.87
API Gravity,	38.6	117.9	80.6	55.7	42.82	34.7	25.5	10.9
Carbon, wt.%		82.5	83.9	86.0	86.1	86.4	86.4	
Hydrogen, wt.%		17.5	16.1	14.0	13.9	13.2	12.8	
Pour point, °C	−12.2				−53.9	−10.6	38.9	56.7
Sulfur, wt.%	0.3675			0.0137	0.058	0.2606	0.6393	1.1302
Nitrogen, ppm	970	0	0	0	2.4	94.6	1346	4553
Viscosity at 20 °C/68 °F, cSt	4.59	0.41	0.46	0.73	1.74	6.76	118.4	1789683
Viscosity at 100 °C/212 °F, cSt	1.35	0.24	0.26	0.38	0.68	1.43	5.91	372
Mercaptan sulfur, ppm	25			22.8	35.3			
CCR, wt.%	1.71					0	0.11	14.21
Nickel, ppm	1.7					0	0.1	12.8
Vanadium, ppm	5.2					0	0.1	41.5
Heat of Combustion (Gross), BTU/lb	19701							
Heat of Combustion (Net), BTU/lb	18496	19078	18729	18561	18546			
Salt content, lb per thousand barrel	1.7							
Paraffins, vol.%		100	84.77	46.64	48.83	39.42	30.18	
Naphthenes, vol.%		0	13.85	36.56	31.54	37.44	31.83	
Aromatics, vol.%				16.8	15.15			

Table 1.1 (continued)

	Whole crude	C4 and C4 –	C5–74 °C	74–166 °C	166–480 °C	480–249 °C	249–537 °C	537 °C+
Freeze point, °C					−43.9	−0.6		
Smoke point, mm					23.3			
Cetane Index 1990 (D4737)	37	131	44	30	43	55	59	43
Cloud point, °C					−47.8	−3.9		
Aniline pt, °C					57.7	69.5	87.1	
Distillation type	D1160	D86	D86	D86	D86	D86	D1160	D1160
ASTM IBP, °C	0.2	−70.9	−57.2	206.9	97.2	263.1	365.2	559.1
5 vol.%, °C	51.9	−27.3	−32.9	212.1	100.1	265.6	367.8	561.7
10 vol.%, °C	79.7	13.8	−10.1	214.8	101.6	266.7	373.1	565.7
20 vol.%, °C	119.9	30.2	−1.0	220.8	104.9	269.7	384.1	575.1
30 vol.%, °C	160.7	36.8	2.7	227.6	108.7	273.7	396.7	585.8
40 vol.%, °C	205.6	38.2	3.4	235.8	113.2	278.4	410.8	598.2
50 vol.%, °C	254.3	38.3	3.5	244.1	117.8	283.2	426.3	612.4
60 vol.%, °C	308.7	42.7	5.9	254.1	123.4	288.7	442.8	631.2
70 vol.%, °C	364.0	46.5	8.1	265	129.4	294.8	459.5	653.1
80 vol.%, °C	425.6	49.3	9.6	276.8	136.0	301.4	477.6	681.3
90 vol.%, °C	502.9	47.5	8.6	289.4	143.0	308.3	496.0	718.7
95 vol.%, °C	570.9	47.1	8.4	296.4	146.9	312.2	507.4	751.0
ASTM EBP, °C	730.7	47.9	8.8	307.7	153.2	318.2	520.7	791.6

A typical crude assay includes two types of information for an oil sample: (1) *bulk properties*; and (2) *fractional properties*. Table 1.1 gives examples of both properties of a crude assay. For design and modeling purposes, it is always the best practice to have process data obtained in the same period as assay data, since the properties and composition of crude change over time as it is produced from a given well. Kaes [1] suggests that assay data should not be two years older than the process data used to build process simulation. We explain both bulk and fractional properties in the following subsections.

1.1.1
Bulk Properties

Bulk properties include specific gravity, sulfur content, nitrogen content, metal (Ni, V, Fe etc.) content, asphaltene content, C/H ratio, pour point, flash point, freeze point, smoke point, aniline point, cloud point,viscosity, carbon residue, light hydrocarbon yields (C1–C4), acid number, refractive index and boiling point curve. We generally use the *API (American Petroleum Institute) gravity* to specify the specific gravity (SG) of the crude oil as API = (141.5/SG) – 131.5. SG is the specific gravity defined as the ratio of the density of the crude oil to the density of water both at 15.6 °C (60 °F). The API gravity varies from less than 10 for very heavy crudes, to between 10 and 30 for heavy crudes, to between 30 and 40 for medium crudes, and to above 40 for light crudes.

The *sulfur content* is expressed as a percentage of sulfur by weight, and varies from less than 0.1% to greater than 5%. Crude oils with less than 1 wt.% sulfur are called low-sulfur or sweet crude, and those with more than 1 wt.% sulfur are called high-sulfur or sour crude. Sulfur-containing constituents of the crude oil include simple mercaptans (also known as thiols), sulfides, and polycyclic sulfides. *Mercaptan sulfur* is simply an alkyl chain (R–) with –SH group attached to it at the end. The simplest form of R–SH is methyl mercaptan, CH_3SH.

The *pour point* is a measure of how easy or difficult to pump the crude oil, especially in cold weather. Specifically, the pour point is the lowest temperature at which a crude oil will flow or pour when it is chilled without disturbance at a controlled rate. The pour point of the whole crude or oil fractions boiling above 232 °C (450 °F) is determined by the standard test ASTM D97.

The *flash point* of a liquid hydrocarbon or an oil fraction indicates its fire and explosion potential, and it is the lowest temperature at which sufficient vapor is produced above the liquid to form a mixture with air that a spontaneous ignition can occur if a spark is present. One of the standard ASTM test methods for the flash point is D3278.

The *freeze point* is the temperature at which the hydrocarbon liquid solidifies at atmospheric pressure. It's an important property for kerosene and jet fuels, because of the very low temperatures encountered at high altitudes in jet planes. One of the standard test methods for the freeze point is ASTM D4790.

The *smoke point* refers to the height of a smokeless flame of fuel in millimeters beyond which smoking takes places. It reflects the burning quality of

kerosene and jet fuels, and is determined by the standard testing method ASTM D1322.

The *aniline point* represents the minimum temperature for complete miscibility of equal volumes of aniline and petroleum oil. It's an important property of diesel fuels, and is measured by ASTM D611.

The *cloud point* refers to the temperature at which solidifiable components (waxes) present in the oil sample begin to crystallize or separate from solution under a method of prescribed chilling. It's an important specification of middle distillate fuels, as determined by ASTM D2500.

The *Conradson carbon residue (CCR)* results from ASTM test D189. It measures the coke-forming tendencies of oil. It is determined by destructive distillation of a sample to elemental carbon (coke residue), in the absence of air, expressed as the weight percentage of the original sample. A related measure of the carbon residue is called *Ramsbottom carbon residue*. A crude oil with a high CCR has a low value as a refinery feedstock.

The *acid number* results from ASTM test method D3339-11 that determines the organic acidity of a refinery stream.

The *refractive index* represents the ratio of the velocity of light in a vacuum to that in the oil. It is determined by ASTM D1218.

The *gross heat of combustion or high heating value (HHV)* is the amount of heat produced by the complete combustion of a unit quantity of fuel. We obtain the gross heat of combustion by cooling down all products of the combustion to the temperature before the combustion, and by condensing all the water vapor formed during combustion.

The *net heat of combustion or lower heating value (LHV)* is obtained by subtracting the latent heat of vaporization of the water vapor formed by the combustion from the gross heat of combustion or higher heating value.

The *true boiling point (TBP) distillation* [1] of a crude oil or petroleum fractions results from using the U. S. Bureau of Mines Hempel method and the ASTM D-285 test procedure. Neither of these methods specifies the number of theoretical stages or the molar reflux ratio used in the distillation. Consequently, there is a trend toward applying a 15 : 5 distillation according to ASTM D2892, instead of the TBP. The 15 : 5 distillation uses 15 theoretical stages and a molar reflux ratio of 5.

A key result from a distillation test is *the boiling point curve*, that is, the boiling point of the oil fraction versus the fraction of oil vaporized. The *initial boiling point (IBP)* is defined as the temperature at which the first drop of liquid leaves the condenser tube of the distillation apparatus. The final boiling point or the *end point (EP)* is the highest temperature recorded in the test.

Additionally, oil fractions tend to decompose or crack at a temperature of approximately 650 °F (344 °C) at one atmosphere. Thus, the pressure of TBP distillation is gradually reduced to as low as 40 mmHg, as this temperature is approached to avoid cracking the sample and distorting measurements of true components in the oil.

The TBP distillation typically takes much time and labor. In practice, we carry out the distillation test of oil fractions using other less costly ASTM methods and

convert the resulting boiling point curve to TBP curve using correlations, as given in the *API Technical Data Book-Petroleum Refining* [2]. We have implemented these correlations in an Excel spreadsheet of the Interconversion of boiling point curves from typical ASTM distillation methods in a hands-on workshop in Section 1.3.

The *ASTM D86 distillation* of an oil fraction takes place at laboratory room temperature and pressure. Note that the D86 distillation will end below an approximate temperature of 650 °F (344 °C), at which petroleum oils begin to crack at one atmospheric pressure.

The *ASTM D1160 distillation* of an oil fraction is applicable to high-boiling oil samples (e.g. heavy heating oil, cracker gas oil feed, residual oil, etc.) for which there is significant cracking at atmospheric pressures. The sample is distilled at a reduced pressure, typically at 10 mmHg, to inhibit cracking. In fact, at 10 mmHg, we can distill an oil fraction up to temperatures of 950 to 1000 °F (510 to 538 °C), as reported on a 760-mmHg basis. The reduced pressure used for D1160 distillation produces a separation of components that is more ideal than that for D86 distillation.

The ASTM D2887 distillation of an oil fraction is a popular chromatographic procedure to "simulate" or predict the boiling point curve of an oil fraction. We determine the boiling point distribution by injecting the oil sample into a gas chromatograph that separates the hydrocarbons in a boiling-point order. We then relate the retention time inside the chromatograph to the boiling point through a calibration curve.

1.1.2
Fractional Properties

Bulk properties provide a quick understanding of the type of the oil sample such as sweet and sour, light and heavy, etc. However, refineries require *fractional properties* of the oil sample that reflects the property and composition for specific boiling-point range to properly refine it into different end products such as gasoline, diesel and raw materials for chemical process. Fractional properties usually contains paraffins, naphthenes and aromatics (PNA) contents, sulfur content, nitrogen content for each boiling-point range, octane number for gasoline, freezing point, cetane index and smoke point for kerosene and diesel fuels.

The *octane number* is a measure of the knocking characteristics of a fuel in a laboratory gasoline engine according to ASTM D2700 [1]. We determine the octane number of a fuel by measuring its knocking value compared to the knocking of a mixture of n-heptane and isooctane or 2-2-4-trimethylpentane (224TMP). By definition, we assign an octane number of 0 to pure heptane and of 100 to 224TMP. Therefore, a mixture of 30% heptanes and 70% isooctane has an octane number of 70.

There are two specific octane numbers in use. The *motor octane number (MON)* reflects the engine performance at highway conditions with high speeds (900 rpm), while the *research octane number (RON)* corresponds to the low-speed city driving

(600 rpm). RON is typically higher than MON because of engine test efficiencies. The posted octane number is an average of MON and RON.

The *cetane number* measures the ease for self-ignition of a diesel fuel sample and is essentially an opposite of the octane number. It represents the percentage of pure cetane (n-hexadecane) in a blend of cetane and alpha methyl-naphthalene that matches the ignition quality of a diesel fuel sample. This quality is important for middle distillate fuels.

The *cetane index* is a number calculated from the average boiling point and gravity of a petroleum fraction in the diesel fuel boiling range, which estimates the cetane number of the fraction according to ASTM D976 (see, for example, http://www.epa.gov/nvfel/testproc/121.pdf).

1.1.3
Interconversion of Distillation Curves

While building a refining process simulation, distillation curve of the oil sample is the most confusing information among assay data since there are different methods used to obtain volatility characteristics of an oil sample. The most widely used tests of distillation curve are ASTM D86, ASTM D1160 (atmospheric distillation), ASTM D1160 (vaccum distillation), ASTM D2887 (chromatographic simulation) and true boiling point (TBP). API Technical Databook [35] presents the characteristics of each test and gives the correlations to perform interconver-

| 760 mmHg | | 760 mmHg | 760 mmHg | 760 mmHg | | 760 mmHg | 760 mmHg | 760 mmHg | 760 mmHg |
ASTM-D86 (C)	Vol. %	ASTM-D86 (F)	TBP (F)	TBP (C)		TBP (C)	TBP (F)	ASTM-D86 (F)	ASTM-D86 (C)
160.0	0%	320	259.1	126.2		126.2	259.1	320	160.0
176.7	10%	350	316.5	158.1		158.1	316.5	350	176.7
193.3	30%	380	372.6	189.2		189.2	372.6	380	193.3
206.7	50%	404	411.2	210.7		210.7	411.2	404	206.7
222.8	70%	433	451.2	232.9		232.9	451.2	433	222.8
242.8	90%	469	496.7	258.2		258.2	496.7	469	242.8
248.9	100%	480	503.0	261.7		261.7	503.0	480	248.9

| | | | 760 mmHg | 760 mmHg | | 760 mmHg | 760 mmHg | | |
ASTM-D2887(C)	Wt%/Vol%	ASTM-D2887(F)	TBP (F)	TBP (C)		TBP (C)	TBP (F)	ASTM-D2887 (F)	ASTM-D2887(C)
145.0	5%	293	322.2	161.2		348.0	658.4	639.1711023	337.3
151.7	10%	305	327.7	164.3		369.0	696.2	685.3443333	363.0
162.2	30%	324	332.4	166.9		406.0	762.8	756.2204757	402.3
168.9	50%	336	336.0	168.9		433.0	811.4	811.4	433.0
173.3	70%	344	339.6	170.9		459.0	858.2	861.2301007	460.7
181.7	90%	359	350.1	176.7		495.0	923.0	922.5542047	494.8
187.2	95%	369	357.4	180.8		512.0	953.6	974.5478925	523.6
198.9	100%	390	366.2	185.7		556.0	1032.8	1038.378625	559.1

| | | | 760 mmHg | 760 mmHg | | 760 mmHg | 760 mmHg | | |
ASTM-D2287 (C)	Wt%/Vol. %	ASTM-D2287 (F)	ASTM-D86 (F)	ASTM-D86 (C)		ASTM-D86 (C)	ASTM-D86 (F)	ASTM-D2887 (F)	ASTM-D2287 (C)
25.0	0%	77	121.3	49.6		298.8	569.9	446.4892018	230.3
33.9	10%	93	128.2	53.5		349.7	661.5	605.3731877	318.5
64.4	30%	148	154.8	68.2		392.0	737.5	715.3377437	379.6
101.7	50%	215	206.3	96.8		424.2	795.5	787.7262099	419.8
140.6	70%	285	270.6	132.5		459.0	858.2	856.5298061	458.1
182.2	90%	360	334.0	167.8		514.5	958.0	964.7774337	518.2
208.9	100%	408	367.5	186.4		577.9	1072.2	1273.441992	689.7

| 760 mmHg | | 760 mmHg | 760 mmHg | 760 mmHg | | 760 mmHg | 760 mmHg | 760 mmHg | 760 mmHg |
ASTM-D1160 (C)	Vol%	ASTM-D1160 (F)	TBP (F)	TBP (C)		TBP (C)	TBP (F)	ASTM-D1160 (F)	ASTM-D1160 (C)
369.0	10%	696.2	686.2	363.4		143.1	289.5	300.1	149.0
406.0	30%	762.8	757.9	403.3		201.5	394.7	400.1	204.5
433.0	50%	811.4	811.4	433.0		246.1	475.0	475.0	246.1
459.0	70%	858.2	857.9	458.8		287.7	549.9	550.0	287.8
495.0	90%	923	922.5	494.7		343.3	650.0	650.0	343.4

Figure 1.1 Conversion spreadsheet for distillation curves.

sion among these ASTM distillation types. Most commercial process simulators include the capability to convert one type of distillation curve to the other. We develop a MS Excel spreadsheet which automates the API conversion between any two of the ASTM distillation types (see Figure 1.1). Section 1.3 presents a hands-on workshop for this interconversion of distillation-curve data.

1.2
Pseudocomponent Generation Based on Boiling-Point Ranges

To simulate refining processes, the first task is to construct a pseudocomponent scheme to characterize the feedstock. Data requirement and definition of the pseudocomponents depend on the type of the refining process to be modeled. There are different concerns to be addressed when building pseudocomponents for fractionation and reaction units. The pseudocomponents for fractionation units have to accurately characterize volatilities of the hydrocarbons in the feedstock in order to calculate vapor-liquid-equilibrium in distillation columns. Therefore, refiners use pseudocomponents based on boiling-point ranges to represent the feedstock and model fractionation units. For modeling of reaction units, refiners partition the hydrocarbons into multiple lumps (or model compounds) based on molecular structure or/and boiling-point ranges, and assume the hydrocarbons of each lump to have an identical reactivity in order to develop the reaction kinetics for reaction units. This section deals with pseudocomponent generation based on boiling-point ranges for fractionation units. Chapters 4 to 6 will present the pseudocomponent schemes for the three major reaction units in modern refinery – fluid catalytic cracking (FCC), catalytic reformer and catalytic hydrocracker.

Most commercial process simulators include the capability to generate pseudocomponents based on boiling-point ranges representing the oil fractions. Workshop 1.4 will demonstrate how to use Aspen HYSYS to generate pseudo-components based on boiling-point ranges for a given oil fraction with required analysis data. Conventionally, there are four steps to develop pseudocomponents based on boiling-point ranges to represent petroleum fraction:

1. Convert ASTM D86/ASTM D1160/ASTMD2887 into TBP curve if TBP curve is not available:
   – We develop a spreadsheet which allows interconversion between different ASTM distillation types based on the correlations from [2] (see Figure 1.1);

2. Cut the entire boiling range into a number of cut-point ranges which are used to define pseudocomponents (see Figure 1.2):
   – The determination of number of cuts is arbitrary. Table 1.2 lists the typical boiling-point ranges for pseudocomponents in commercial simulators.

3. Estimate the density distribution of pseudocomponents if only the bulk density is available:
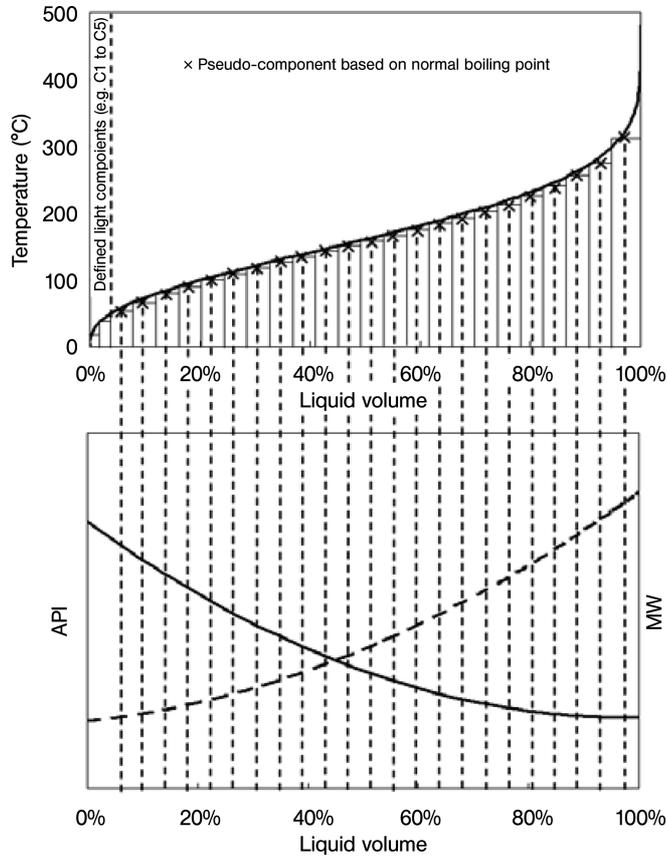
Figure 1.2 Relationship between pseudocomponent properties and the TBP curve (redraw from [1]).

Table 1.2 Typical boiling-point ranges for pseudocomponents in commercial process simulators.

Boiling-point Range	Suggested Number of Pseudocomponents
IBP to 800 °F (425 °C)	30
800 °F to 1200 °F (650 °C)	10
1200 °F to 1650 °F (900 °C)	8

– Assume the UOP or *Watson-Murphy "characterization factor" or K factor* to be constant throughout the entire boiling range and calculate *mean-average boiling point (MeABP)*. Dissimiliar to *weight-average boiling point (WABP)*, MeABP is defined as the average of *molal-average boiling point (MABP)* and *cubic-average boiling point (CABP)*. The following equations define these four boiling-point indicators:

$$\text{WABP} = \sum_{i=1}^{n} x_i \, T_{bi} \tag{1.1}$$

$$\text{MABP} = \sum_{i=1}^{n} x_i \, T_{bi} \tag{1.2}$$

$$\text{CABP} = \left(\sum_{i=1}^{n} x_i \, T_{bi}^{1/3} \right)^3 \tag{1.3}$$

$$\text{MeABP} = \frac{\text{MABP} + \text{CABP}}{2} \tag{1.4}$$

where T_{bi} indicates boiling point of component i and x_i in Equation (1.1) to (1.3) indicate weight fraction, molar fraction and volume fraction of component i, respectively. Here, we create a spreadsheet tool (see Figure 1.3) to perform the iteration of estimating MeABP based on the methods presented by Bollas et al. [3]

$$K_{avg} = \left[\text{MeABP} \right]^{0.333} \Big/ \text{SG}_{avg} \tag{1.5}$$

where K_{avg} is Watson K factor and SG_{avg} is the bulk specific gravity 60 °F/60 °F
– Calculate the density distribution of the entire boiling range:

$$\text{SG}_i = \left[T_{i,b} \right]^{0.333} \Big/ K_{avg} \tag{1.6}$$

where SG_i is the specific gravity 60 °F/60 °F of pseudocomponent i and $T_{i,b}$ is the normal boiling point of pseudocomponent i.

4. Estimate the molecular weight distribution of the entire boiling range if not available and required properties for modeling purpose (see Section 1.3 for details).
Lacking the analysis data of high boiling-point range (> 570 °C) is a common problem while building pseudocomponents based on boiling-point ranges. Therefore, we need to extrapolate the incomplete distillation curve in order to cover the entire boiling-point range. Least-squares and probability-distribution functions are most widely used to perform the extrapolation of distillation curve in most commercial process simulators. Sanchez et al. [5] present a comprehensive review of using probability-distribution functions to fit distillation curves of petroleum fractions. They conclude that the cumulative beta function (with four parameters) can represent a wide range of petroleum products. The beta cumulative density function is defined as:

$$f\left(x, \alpha, \beta, A, B\right) = \int_{A}^{x \leq B} \left(\frac{1}{B-A} \right) \frac{\Gamma\left(\alpha+\beta\right)}{\Gamma\left(\alpha\right)\Gamma\left(\beta\right)} \left(\frac{x-A}{B-A} \right)^{\alpha-1} \left(\frac{B-x}{B-A} \right)^{\beta-1} \tag{1.7}$$

	A	B	C	D
4	TBP Curve @ 760 mmHg			
5	Vol%	Temperature (F)		Initial
6	0	256.8		0
7	10	368.2		5
8	30	447.2		10
9	50	516.9		15
10	70	583.9		20
11	90	633.4		25
12	100	722.2		30
13				35
14	Specific gravity	0.8505		40
15	Refractive index @ 20 C			45
16	Oxygen content (wt%)	0.00		50
17	Initial MeABP (F) [Enter as first guess in yellow cell]	506.76		55
18				60
19	Trial MeABP (F)	497.46		65
20	Trial MeABP (R)	957.13		70
21	Watson-K	11.59		75
22				80
23	Calc. VABP (R)	969.22		85
24	Calc. WABP (R)	972.98		90
25	Calc. MABP (R)	948.85		95
26	Calc. CABP (R)	965.42		
27				
28	Calc. MeABP (R)	957.13		
29				
30	Error (Trial MeABP - Calc. MeABP)	0.00000	(Use goalseek to drive	
31				
32	Correlation for refractive index	A	B	C
33	Naphthas	1.028	0.53	
34	Straight or hydrosulfurized gas oils	0.9734	0.59	
35	Deeply hydrogenated fractions	0.9713	0.59	
36	Short residues	0.9345	0.63	0.006
37	FCC feeds			0.006
38	Coal liquids			0.006
39	Stream cracker residue			
40				
41	Selected correlation			
42				
43				

Naphthas
Straight or hydrosulfurized gas oils
Deeply hydrogenated fractions
Short residues
FCC feeds
Coal liquids
Stream cracker residue

FCC feeds

Figure 1.3 Iteration spreadsheet for MeABP calculation.

where α and β refer to the positive valued parameters that control the shape of the distribution, Γ refers to the standard gamma function, A and B parameters set lower and upper bounds on the distribution and x represents the normalized recovery. We develop a MS Excel spreadsheet to perform the extrapolation of distillation curve by using the cumulative beta distribution function (see Figure 1.4).

Section 1.4 presents a hands-on workshop for applying our spreadsheet to extrapolate an incomplete distillation curve. We note that the density distribution along with boiling point should be used (in step 3) whenever it is available because the assumption of constant Watson *K* factor always fails in low and high boiling-point ranges.

	A	B	C	D	E	F	G	H	I	J	K
1		Beta Distribution									
2	alpha	2									
3	beta	1		Solve							
4	A	0.2									
5	B	0.5									
6				Output of CDF	Input						
7	% Distilled	Temperature		% Distilled	Meas. Theta		Errors	%Distilled	Calculated Theta	Calc. Temp	% Distilled
8	0	351		0	0.3047	0.122	0.014807823	0.00	0.2095	310.1	0.1
9	10	430		0.1	0.4884	0.924	0.678947875	0.05	0.2671	334.8	5
10	20	459		0.2	0.5558	#NUM!	#NUM!	0.10	0.2949	346.8	10
11	30	474		0.3	0.5907	#NUM!	#NUM!	0.30	0.3643	376.7	30
12	40	487		0.4	0.6209	#NUM!	#NUM!	0.50	0.4121	397.2	50
13	50	498		0.5	0.6465	#NUM!	#NUM!	0.70	0.4510	413.9	70
14	90							0.90	0.4846	428.4	90
15	95							0.95	0.4924	431.7	95
16	98							1.00	0.4998	434.9	99.9
17											
18	T_0, ref	220			0.3047		#NUM!				
19	T_1, ref	650			0.6465		#NUM!				
20							#NUM!				

Figure 1.4 Spreadsheet for extrapolating distillation curve.
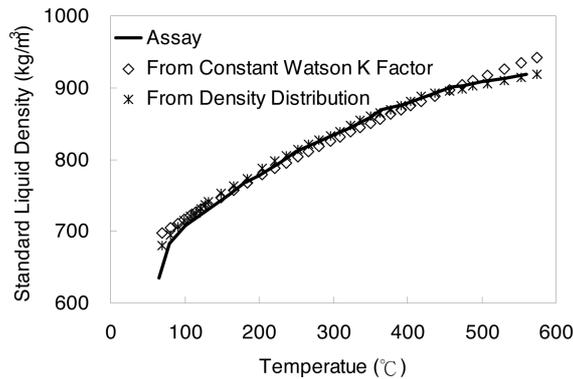
Figure 1.5 Comparison of the pseudocomponents generated from constant Watson *K* factor and density distribution (data obtained from [1]).

Figure 1.5 compares the pseudocomponents generated from constant Watson *K* factor and from density distribution. The pseudocomponents generated from constant Watson *K* factor shows significant deviations from assay data on estimating the densities of pseudocomponents, particularly in both light and heavy ends of the distillation curve. On the other hand, using density distribution is able to provide a good estimation of the densities of pseudocomponents. Estimating the densities of pseudocomponents is the most important part when developing pseudocomponents because density is required for most of the physical property estimations.

1.3
Workshop 1.1 – Interconvert Distillation Curves

There are two situations we may encounter when the distillation curve available is not a TBP curve and needs to be converted – (1) It is another ASTM type; and (2) It is ASTM D1160 at vacuum pressure. The spreadsheet we have developed is able to solve these two cases. The following steps demonstrate how to convert an ASTM D1160 (at 10 mmHg) curve into a TBP curve.

Step 1: Open ASTMConvert.xls.

760 mmHg		760 mmHg	760 mmHg	760 mmHg		760 mmHg	760 mmHg	760 mmHg	760 mmHg
ASTM-D86 (C)	Vol. %	ASTM-D86 (F)	TBP (F)	TBP (C)		TBP (C)	TBP (F)	ASTM-D86 (F)	ASTM-D86 (C)
160.0	0%	320	259.1	126.2		126.2	259.1	320	160.0
176.7	10%	350	316.5	158.1		158.1	316.5	350	176.7
193.3	30%	380	372.6	189.2		189.2	372.6	380	193.3
206.7	50%	404	411.2	210.7		210.7	411.2	404	206.7
222.8	70%	433	451.2	232.9		232.9	451.2	433	222.8
242.8	90%	469	496.7	258.2		258.2	496.7	469	242.8
248.9	100%	480	503.0	261.7		261.7	503.0	480	248.9
			760 mmHg	760 mmHg		760 mmHg	760 mmHg		
ASTM-D2887(C)	Wt%/Vol%	ASTM-D2887 (F)	TBP (F)	TBP (C)		TBP (C)	TBP (F)	ASTM-D2887 (F)	ASTM-D2887(C)
145.0	5%	293	322.2	161.2		348.0	658.4	639.1711023	337.3
151.7	10%	305	327.7	164.3		369.0	696.2	685.3443333	363.0
162.2	30%	324	332.4	166.9		406.0	762.8	756.2204757	402.3
168.9	50%	336	336.0	168.9		433.0	811.4	811.4	433.0
173.3	70%	344	339.6	170.9		459.0	858.2	861.2301007	460.7
181.7	90%	359	350.1	176.7		495.0	923.0	922.5542047	494.8
187.2	95%	369	357.4	180.8		512.0	953.6	974.5478925	523.6
198.9	100%	390	366.2	185.7		556.0	1032.8	1038.378625	559.1
			760 mmHg	760 mmHg		760 mmHg	760 mmHg		
ASTM-D2287 (C)	Wt%/Vol. %	ASTM-D2287 (F)	ASTM-D86 (F)	ASTM-D86 (C)		ASTM-D86 (C)	ASTM-D86 (F)	ASTM-D2887 (F)	ASTM-D2287 (C)
25.0	0%	77	121.3	49.6		298.8	569.9	446.4892018	230.3
33.9	10%	93	128.2	53.5		349.7	661.5	605.3731877	318.5
64.4	30%	148	154.8	68.2		392.0	737.5	715.3377437	379.6
101.7	50%	215	206.3	96.8		424.2	795.5	787.7262099	419.8
140.6	70%	285	270.6	132.5		459.0	858.2	856.5298061	458.1
182.2	90%	360	334.0	167.8		514.5	958.0	964.7774337	518.2
208.9	100%	408	367.5	186.4		577.9	1072.2	1273.441992	689.7
760 mmHg		760 mmHg	760 mmHg	760 mmHg		760 mmHg	760 mmHg	760 mmHg	760 mmHg
ASTM-D1160 (C)	Vol%	ASTM-D1160 (F)	TBP (F)	TBP (C)		TBP (C)	TBP (F)	ASTM-D1160 (F)	ASTM-D1160 (C)
280.8	10%	537.3541391	527.3	275.2		143.1	289.5	300.1	149.0
350.6	30%	663.1131895	657.8	347.7		201.5	394.7	400.1	204.5
402.7	50%	756.9327522	756.9	402.7		246.1	475.0	475.0	246.1
450.5	70%	842.8909373	842.9	450.5		287.7	549.9	550.0	287.8
513.0	90%	955.4507826	955.6	513.1		343.3	650.0	650.0	343.4

Figure 1.6 ASTMConvert.xls.

Step 2: Copy and paste the ASTM D1160 curve into the sheet for interconversion among different testing pressures of ASTM D1160.

Pressure =	30	mmHg	2 =< P =< 760			
X	0.00180742			760 mmHg	760 mmHg	760 mmHg
TBP/D1160 (C)	Vol%	TBP/D1160 (F)	TBP/D1160 (R)	TBP/D1160 (R)	TBP/D1160 (F)	TBP/D1160 (C)
143.1	10%	289.5	749.2	941.7	482.1	250.0
201.5	30%	394.7	854.4	1063.5	603.8	317.7
246.1	50%	475.0	934.7	1154.8	695.1	368.4
287.7	70%	549.9	1009.6	1238.8	779.1	415.1
343.3	90%	650.0	1109.7	1349.2	889.5	476.4

Figure 1.7 Input cells of ASTM D1160 interconversion in ASTMConvert.xls.

Step 3: Input the testing pressure which is 10 mmHg in this case.

47	Pressure =	10	mmHg	2 =< P =< 760			
48	X	0.00195599			760 mmHg	760 mmHg	760 mmHg
49	TBP/D1160 (C)	Vol%	TBP/D1160 (F)	TBP/D1160 (R)	TBP/D1160 (R)	TBP/D1160 (F)	TBP/D1160 (C)
50	143.1	10%	289.5	749.2	997.0	537.4	280.8
51	201.5	30%	394.7	854.4	1122.8	663.1	350.6
52	246.1	50%	475.0	934.7	1216.6	756.9	402.7
53	287.7	70%	549.9	1009.6	1302.6	842.9	450.5
54	343.3	90%	650.0	1109.7	1415.1	955.5	513.0

Figure 1.8 Input pressure for ASTM D1160 interconversion.

Step 4: The blue cells will show the converted results which correspond to ASTM D1160 at 1 atmosphere.

47	Pressure =	10	mmHg	2 =< P =< 760			
48	X	0.00195599			760 mmHg	760 mmHg	760 mmHg
49	TBP/D1160 (C)	Vol%	TBP/D1160 (F)	TBP/D1160 (R)	TBP/D1160 (R)	TBP/D1160 (F)	TBP/D1160 (C)
50	143.1	10%	289.5	749.2	997.0	537.4	280.8
51	201.5	30%	394.7	854.4	1122.8	663.1	350.6
52	246.1	50%	475.0	934.7	1216.6	756.9	402.7
53	287.7	70%	549.9	1009.6	1302.6	842.9	450.5
54	343.3	90%	650.0	1109.7	1415.1	955.5	513.0

Figure 1.9 The results of ASTM D1160 interconversion.

Step 5: Copy the values of ASTM D1160 (at 1 atm) to the sheets for converting ASTM D1160 at 1 atm into TBP.

37	760 mmHg		760 mmHg	760 mmHg	760 mmHg
38	ASTM-D1160 (C)	Vol%	ASTM-D1160 (F)	TBP (F)	TBP (C)
39	280.8	10%	537.3541391	527.3	275.2
40	350.6	30%	663.1131895	657.8	347.7
41	402.7	50%	756.9327522	756.9	402.7
42	450.5	70%	842.8909373	842.9	450.5
43	513.0	90%	955.4507826	955.6	513.1

Figure 1.10 Input cells for other ASTM interconversion in ASTMConvert.xls.

Step 6: The blue cells reveals the converted TBP curve.

37	760 mmHg		760 mmHg	760 mmHg	760 mmHg
38	ASTM-D1160 (C)	Vol%	ASTM-D1160 (F)	TBP (F)	TBP (C)
39	280.8	10%	537.3541391	527.3	275.2
40	350.6	30%	663.1131895	657.8	347.7
41	402.7	50%	756.9327522	756.9	402.7
42	450.5	70%	842.8909373	842.9	450.5
43	513.0	90%	955.4507826	955.6	513.1

Figure 1.11 Result cells for other ASTM interconversion in ASTMConvert.xls.

1.4
Workshop 1.2 – Extrapolate an Incomplete Distillation Curve

Step 1: Open Beta.xls. Cells B2 to B5 show the adjustable parameters in beta distribution function, the cells A8 to B16 require the input of the distillation curve, cells H8 to K16 and the graph indicate the fitted results.
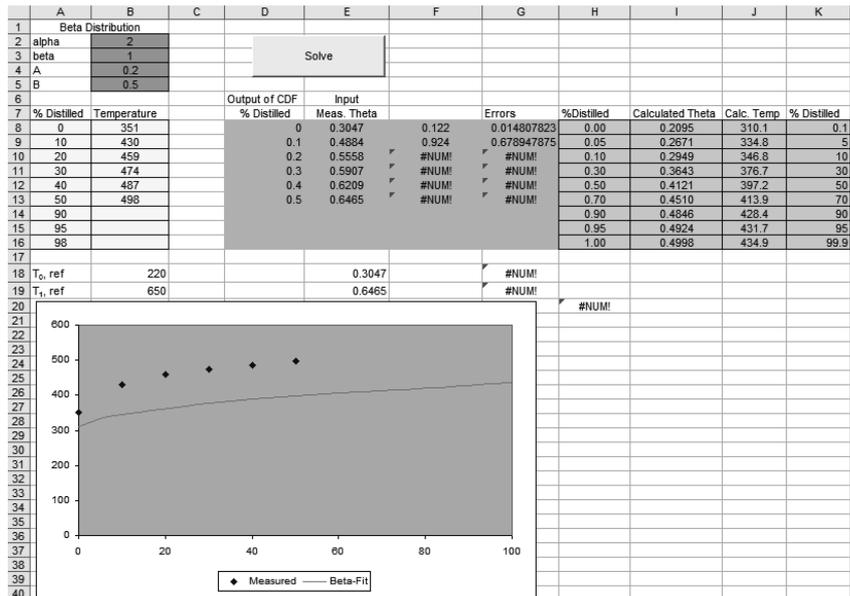
Figure 1.12 Beta.xls.

Step 2: Input the incomplete distillation curve into cells A8 to B16. The user is allowed to add/remove according to the number of points in the distillation curve.
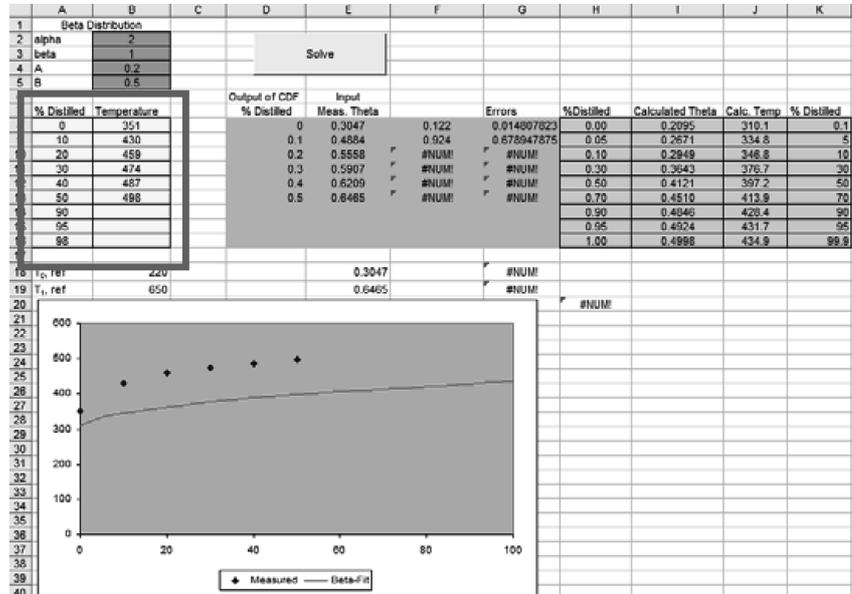
Figure 1.13 Input cells in Beta.xls.

Step 3: Click "solve" to run the fitting program.
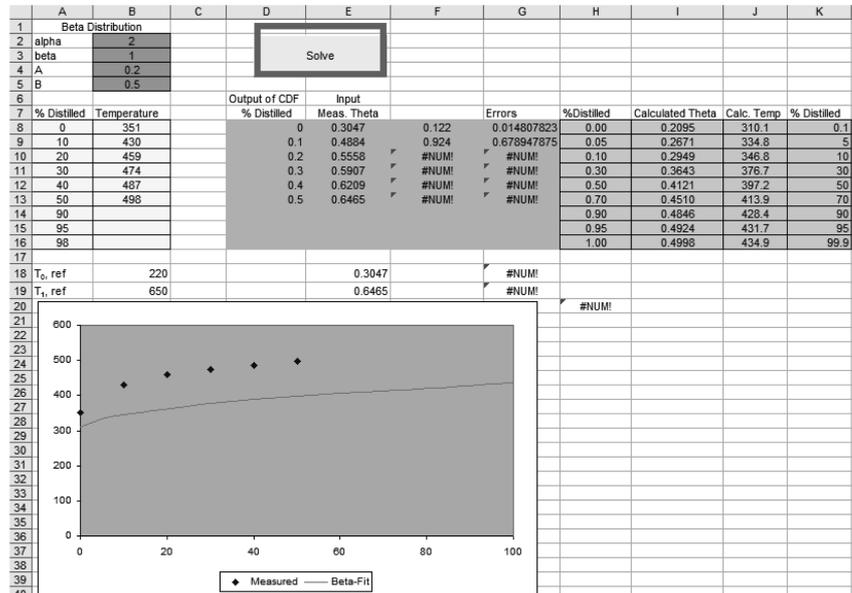
Figure 1.14 Activation button in Beta.xls.

Step 4: The cells B2 to B5 show the fitted parameters. Cells H8 to K16 and the graph represent the extrapolated distillation curve.

	A	B	C	D	E	F	G	H	I	J	K
1		Beta Distribution									
2	alpha	2.55226284			Solve						
3	beta	0.67138015									
4	A	0.28274718									
5	B	0.708745									
6				Output of CDF	Input						
7	% Distilled	Temperature		% Distilled	Meas. Theta		Errors	%Distilled	Calculated Theta	Calc. Temp	% Distilled
8	0	351		0	0.3047	0.000	7.4082E-08	0.00	0.3191	357.2	0.1
9	10	430		0.1	0.4884	0.094	3.2186E-05	0.05	0.4454	411.5	5
10	20	459		0.2	0.5558	0.209	7.7717E-05	0.10	0.4928	431.9	10
11	30	474		0.3	0.5907	0.297	8.3479E-06	0.30	0.5917	474.4	30
12	40	487		0.4	0.6209	0.396	1.6955E-05	0.50	0.6462	497.9	50
13	50	498		0.5	0.6465	0.501	1.8824E-06	0.70	0.6818	513.2	70
14	90							0.90	0.7037	522.6	90
15	95							0.95	0.7070	524.0	95
16	98							1.00	0.7087	524.8	99.9
17											
18	T_0, ref	220			0.3047		0.00013716				
19	T_1, ref	650			0.6465		2.286E-05				
20							7.772E-05				

Figure 1.15 Fitted results in Beta.xls.

1.5
Workshop 1.3 – Calculate MeABP of a Given Assay

Step 1: Open MeABP Iteration.xls.

Figure 1.16 MeABP.xls.

Step 2: Select the type of the oil fraction. We choose naphtha in this case.

35	Deeply hydrogenated fractions	0.9713	0.59
36	Short residues	0.9345	0.63
37	FCC feeds	0.9365	0.63
38	Coal liquids	0.9448	0.63
39	Stream cracker residue	0.881	0.7
40			
41	Selected correlation	5	
42			
43		FCC feeds	
44		Naphthas	
45		Straight or hydrosulfurized gas oils	
46		Deeply hydrogenated fractions	
47		Short residues	
48		FCC feeds	
49		Coal liquids	
50		Stream cracker residue	
51			

Figure 1.17 Select oil type.

Step 3: Input TBP curve and specific gravity in highlighted cells.

	Vol%	Temperature (F)
5	Vol%	Temperature (F)
6	0	310.2
7	10	341.3
8	30	369.8
9	50	387.4
10	70	406.4
11	90	433.4
12	100	480.6
13		
14	Specific gravity	0.7457
15	Refractive index @ 20 C	
16	Oxygen content (wt%)	0.00
17	Initial MeABP (F) [Enter as first guess in yellow cell]	384.93

Figure 1.18 Input distillation curve and specific gravity.

Step 4: Go to Tool/Goal Seek.
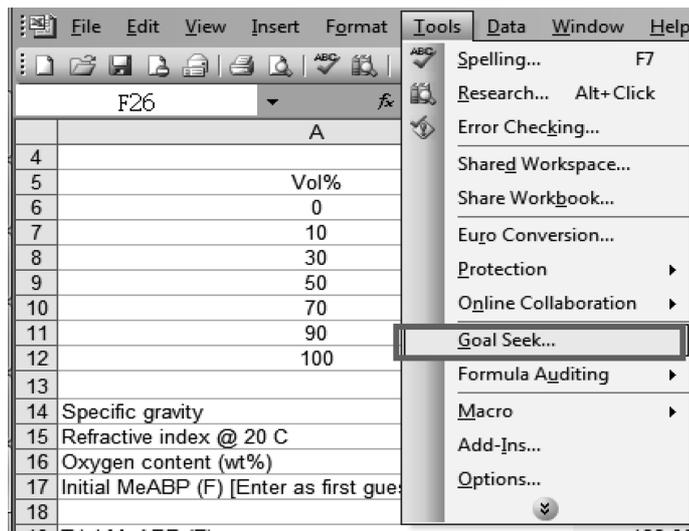
Figure 1.19 Activate "goal seek" in Beta. slx.

Step 5: Assign cell 19 to "By changing cell" and cell B30 to "Set cell" and input "0" in "To value". And then, click "OK".

18				60	65
19	Trial MeABP (F)	422.00		65	70
20	Trial MeABP (R)	881.67		70	75
21	Watson-K	12.86			
22					
23	Calc. VABP (R)	847.70			
24	Calc. WABP (R)	848.19			
25	Calc. MABP (R)	845.17			
26	Calc. CABP (R)	847.21			
27					
28	Calc. MeABP (R)	846.19			
29					
30	Error (Trial MeABP - Calc. MeABP)	1258.74304	(Use goalseek to drive green cell to 0 by c		

Goal Seek

Set cell: B30

To value: 0

By changing cell: B19

OK   Cancel
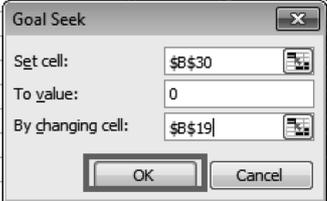
Figure 1.20 Assign tuning and objective cells.

Step 6: Row 28 reveals the calculated MeABP for the given oil fraction.

		Vol%	Temperature (F)
5		Vol%	Temperature (F)
6		0	310.2
7		10	341.3
8		30	369.8
9		50	387.4
10		70	406.4
11		90	433.4
12		100	480.6
13			
14	Specific gravity		0.7457
15	Refractive index @ 20 C		
16	Oxygen content (wt%)		0.00
17	Initial MeABP (F) [Enter as first guess in yellow cell]		384.93
18			
19	Trial MeABP (F)		386.55
20	Trial MeABP (R)		846.22
21	Watson-K		12.68
22			
23	Calc. VABP (R)		847.70
24	Calc. WABP (R)		848.19
25	Calc. MABP (R)		845.19
26	Calc. CABP (R)		847.21
27			
28	Calc. MeABP (R)		846.20
29			
30	Error (Trial MeABP - Calc. MeABP)		0.00042

Figure 1.21 Iterative MeABP in MeABP.xls.

1.6
Workshop 1.4 – Duplicate the Oil Fraction in Aspen HYSYS Petroleum Refining

Step 1: Start a new case in Aspen HYSYS Petroleum Refining.

Figure 1.22 Start a new case in Aspen HYSYS Petroleum Refining.

Step 2: Click "add" to add a new component list.
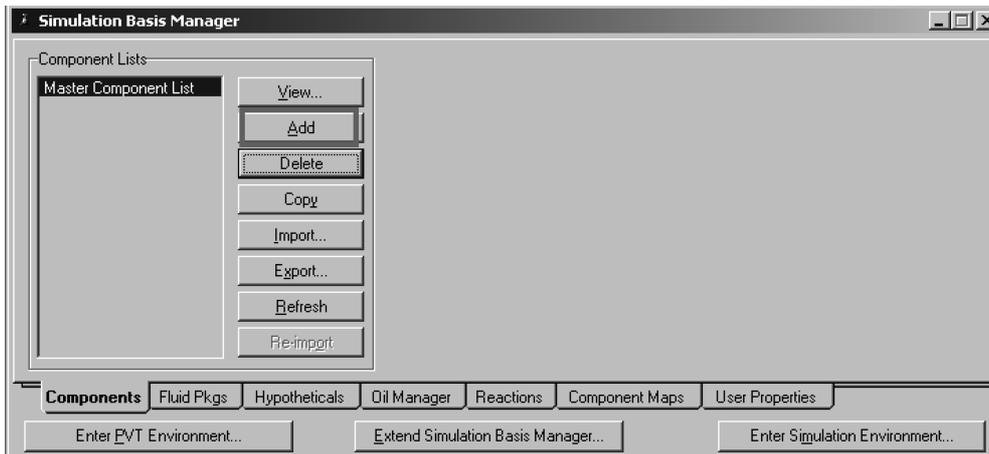
Figure 1.23 Add a new component list.

Step 3: Click "view" to edit the component list. Add light components which are shown in assay data.
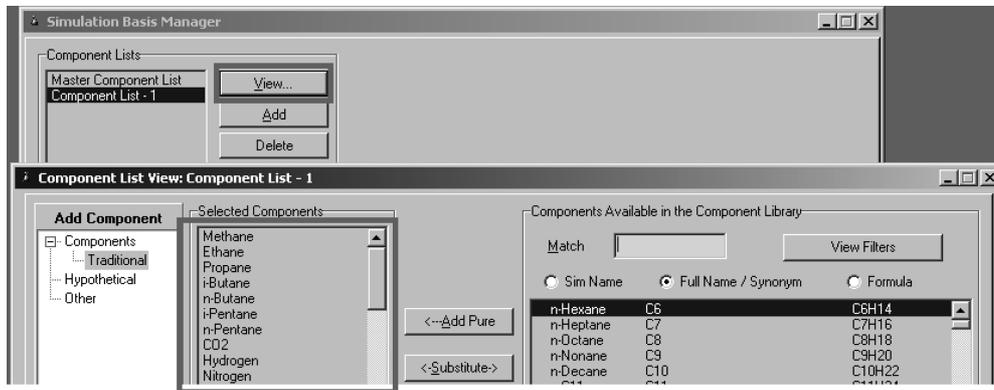
Figure 1.24 Add light components.

Step 4: Click "add" in "fluid pkgs" tab to add the thermodynamic model.
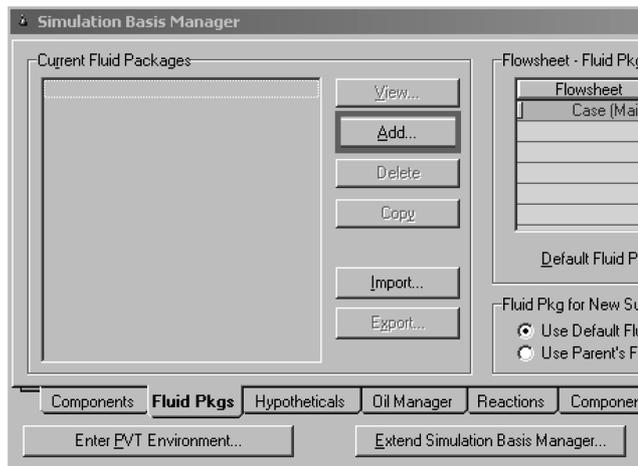
Figure 1.25 Enter the list of thermodynamics models.

Step 6: Select the Peng-Robinson method.
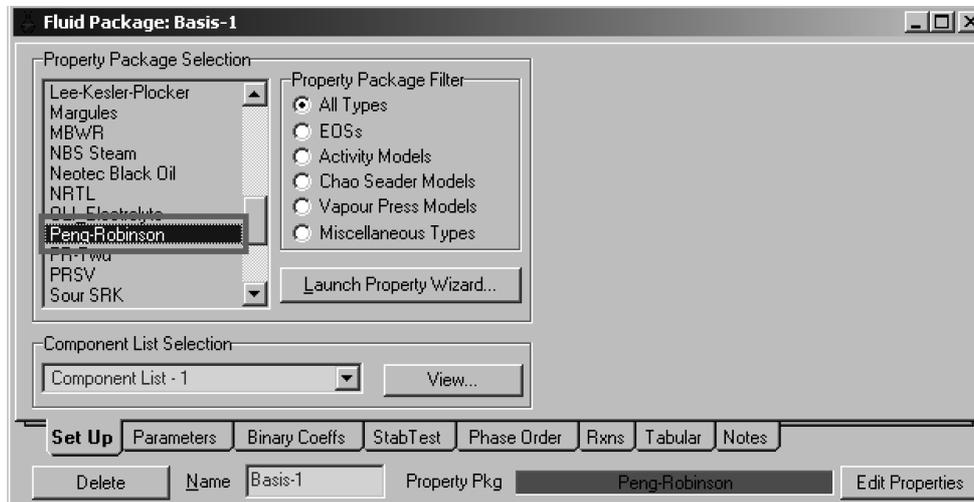
Figure 1.26 Select a thermodynamics model.

Step 7: Click "enter oil environment" in "oil manager" tab.
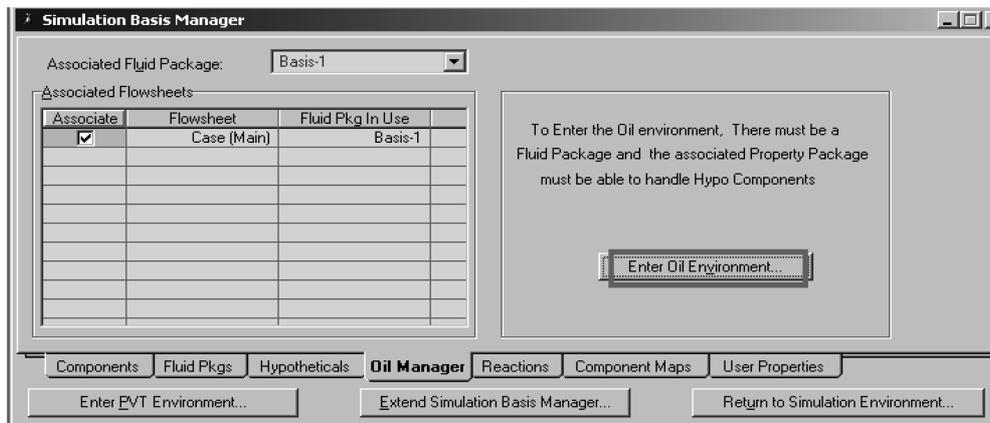
Figure 1.27 Enter the "oil environment".

Step 8: Click "add" to add a new assay and click "view" to edit the assay data.
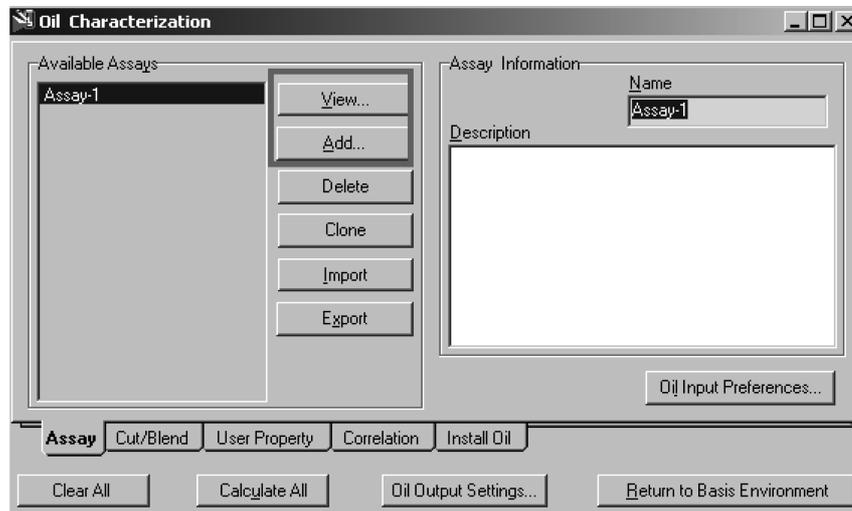
Figure 1.28 Add and edit assay data.

Step 9: In this case, we have TBP curve, bulk density and light end composition. Therefore, we use these three properties to build the assay in Aspen HYSYS Petroleum Refining. Users are allowed to input molecular weight curve, density curve and viscosity curve if available.
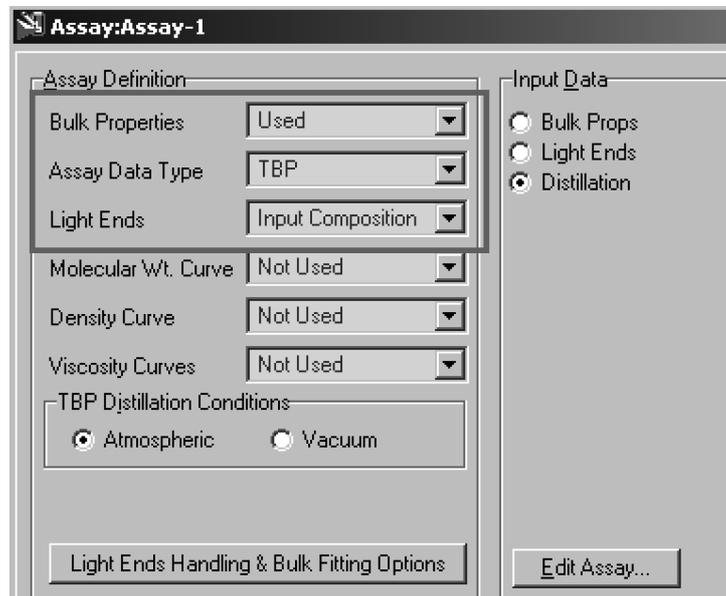
Figure 1.29 Select the data to be used to define an assay.

Step 10: Check "distillation" and click "edit assay" to input the distillation curve.
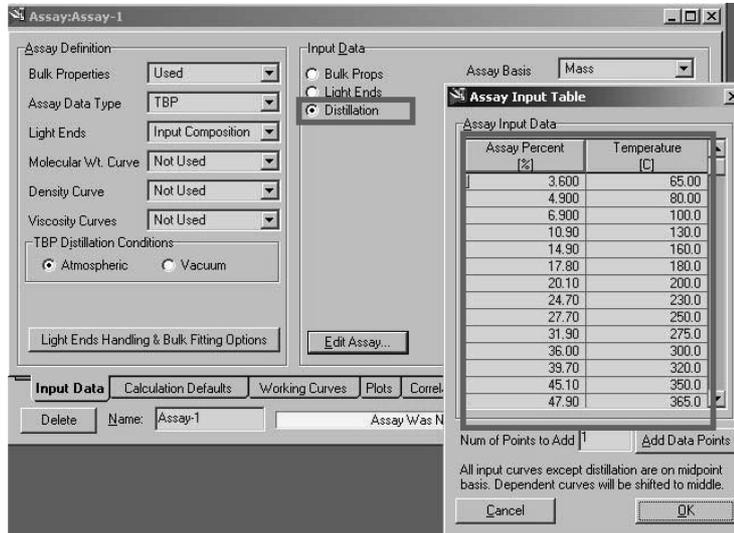
Figure 1.30 Enter the distillation curve.

Step 11: Check "bulk props" to input the bulk density and other bulk properties if available.
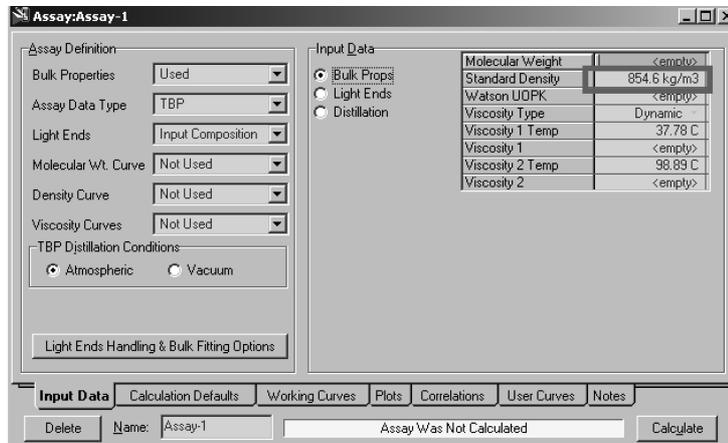
Figure 1.31 Enter the bulk density.

Step 12: Check "light ends" to input the light-end composition.

Figure 1.32 Enter the composition of light components.

Step 13: Click "calculate" to enable the Aspen HYSYS Petroleum Refining's calculation for working curves which are used to generate pseudocomponents.

Figure 1.33 Enable the pseudocomponent generation.

Step 14: Go to "cut/blend" tab and click "add" to add a new cut. Then, click "view" to edit the cut.
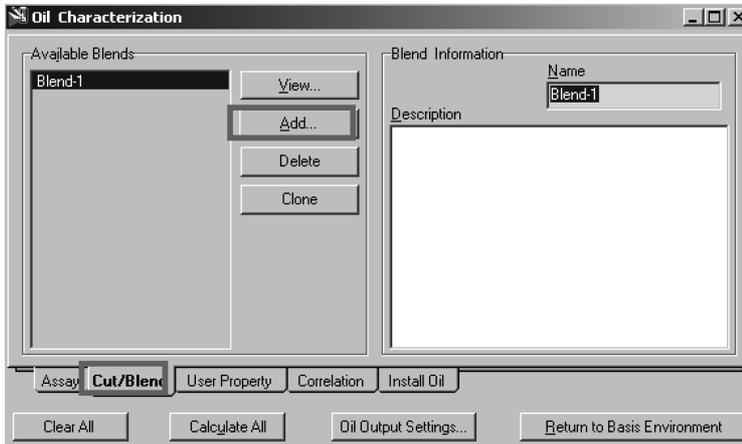
Figure 1.34 Add cut/blend.

Step 15: Select "assay-1" and click "add" to use the assay we input to generate the corresponding pseudocomponents.
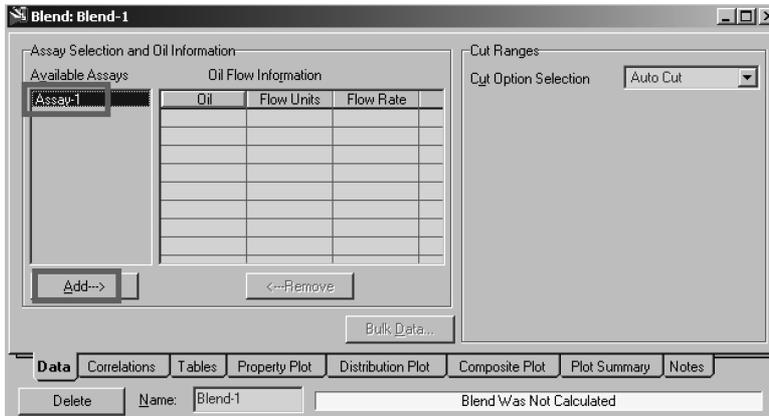
Figure 1.35 Select the assay used to be cut or blended.

Step 16: Go to "table" tab to check the generated pseudocomponents.

Figure 1.36 The pseudocomponents used to represent the cut or blend.

Step 17: Close the window in previous step. And then, go to "install oil" tab, check "install" box and enter stream name (it is oil in this case).

Figure 1.37 Install the cut/blend into simulation.

Step 18: Click "return to basis environment".
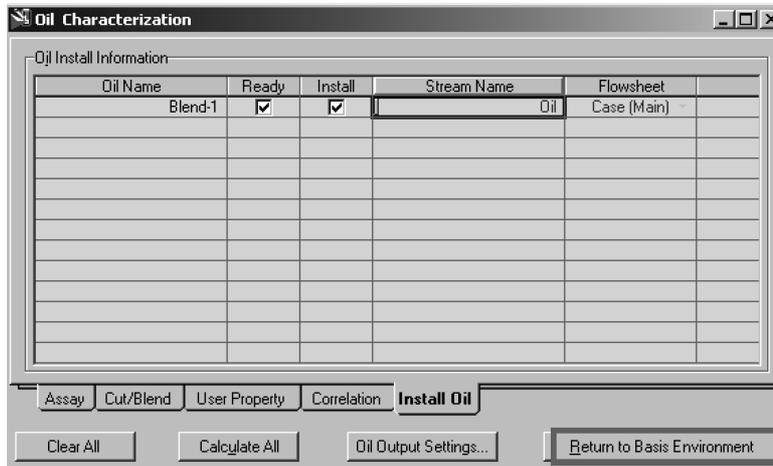
Figure 1.38 Return to the basis environment.

Step 19: Click "return to simulation environment".
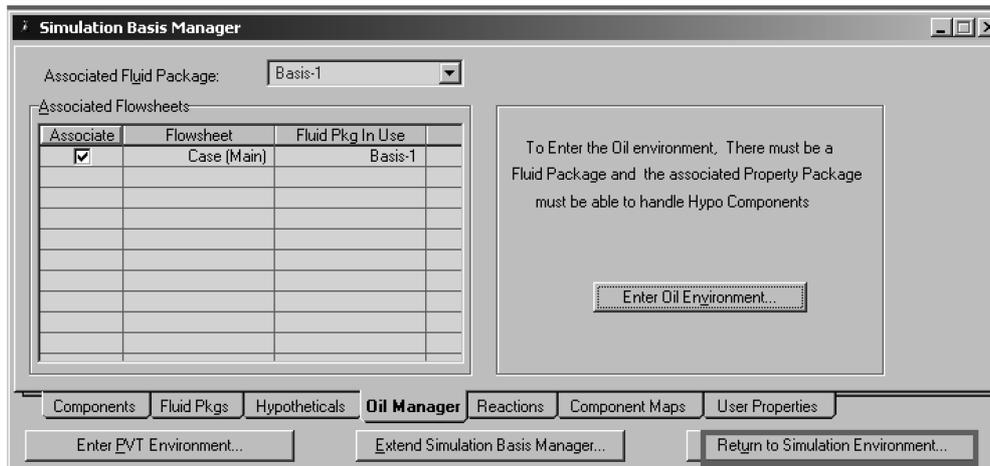
Figure 1.39 Return to the simulation environment.

Step 20: The oil fraction is duplicated in Aspen HYSYS Petroleum Refining.
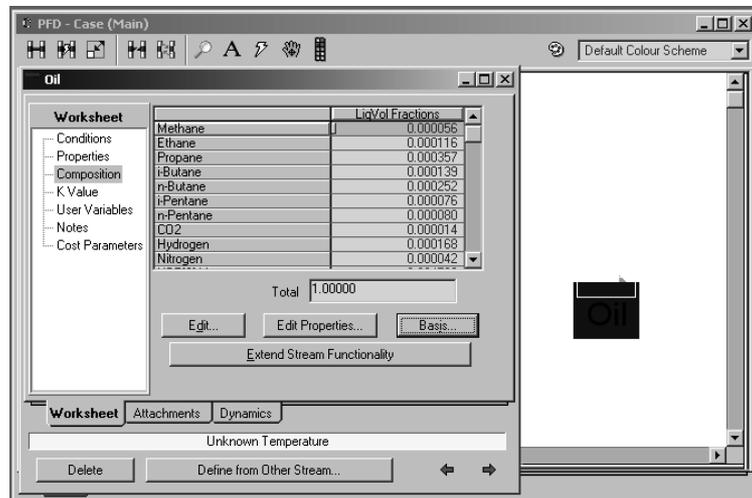
Figure 1.40 The stream in the simulation environment used to represent the oil fraction.

1.7
Property Requirements for Refinery Process Models

We classify the processes in modern refinery into two categories: separation units and reaction units. To develop a process model for any unit, we need to check mass and energy balances of the flowsheet and perform calculations to describe the performance of the target unit. Therefore, the essential properties (physical and chemical) used to simulate these processes depend on the target unit, the chosen pseudocomponent scheme and the selected kinetic model for reaction unit. Chapters 4 through 6 will represent the relevant issues for the three major reaction units in a modern refinery – FCC, catalytic reformer and hydrocracker. While this chapter focuses primarily on the thermophysical properties required for modeling fractionation processes, the general framework for developing these properties for different kinds of pseudocomponents (i.e. those generated by kinetic lumping networks) is the same.

The previous sections in this chapter address the creation of pseudocomponents by cutting an assay curve into a set of discrete components based on boiling-point ranges. We also briefly alluded to physical properties and process thermodynamics selection in the earlier workshops of this chapter. In this section, we consider, in detail, the problem of how to represent these components in the process modeling software. There are two major concerns in this area: physical properties of pseudocomponents and selection of a thermodynamic system that can deal with these hydrocarbon pseudocomponents in the context of refinery modeling.

A correct selection of physical properties and process thermodynamics results in a process model that can accurately account for material and energy flows in both vapor and liquid process streams.

1.8
Physical Properties

For any process simulation that involves only vapor-liquid phases, certain key physical and thermodynamic properties must be available for each phase. Table 1.3 lists these properties for all phases. We can typically obtain these properties for pure components (i.e. n-hexane, n-heptane, etc.) from widely available databases such as DIPPR [2]. Commercial process simulation software (including Aspen HYSYS) also provides a large set of physical and thermodynamic properties for a large number of pure components. However, using these databases requires us to identify a component by name and molecular structure first, and use experimentally measured or estimated values from the same databases. Given the complexity of crude feed, it is not possible to completely analyze the crude feed in terms of pure components. Therefore, we must be able to estimate these properties for each pseudocomponent based on certain measured descriptors.

It is important to note the properties given in Table 1.3 are the minimal physical properties required for rigorous accounting of the material and energy flows in the process. As we will discuss in the subsequent sections, process models may require additional properties (especially vapor pressure) depending on the type of thermodynamic models being considered.

Table 1.3 Required properties for each phase.

Phase	Required Properties
Vapor	Ideal Gas Heat Capacity (CP_{IG})
Liquid	Liquid Heat Capacity (CP_L), Liquid Density (ρ_L), Latent Heat of Vaporization (ΔH_{VAP}), Vapor Pressure (P_{VAP})
Both	Molecular weight (MW)

1.8.1
Estimating Minimal Physical Properties for Pseudocomponents

We show in previous sections that the minimal amount of information to create pseudocomponents is a distillation curve and a specific gravity or density distribution. If only the bulk density is available, we can use the constant Watson *K*-Factor assumption to estimate the density distribution. If only a partial density distribution is available, we can use the beta function to extrapolate an incomplete

distillation curve. Note that it is almost always better to incorporate as much experimentally measured information about the density curve as possible when building the process model. Once the distillation and density curve are available, we can cut the curve into a set of discrete pseudocomponents, each with its own boiling point and density. We will use these two measured properties to estimate a variety of different types of physical properties (i.e. molecular weight, critical temperature, critical pressure, acentric factor, etc.). Using these estimated physical properties, we can derive additional estimates for minimal physical properties required for process simulation. We have also provided a Microsoft Excel spreadsheet in the material that accompanies this text which includes many of the correlations given in this section.

1.8.2
Molecular Weight

The molecular weight is the most basic information for a given pseudocomponent. Molecular weight is a required property to ensure an accurate material balance throughout the process flowsheet. Researchers have studied extensively the trends of molecular weight for a variety of pure hydrocarbons and oil fractions. There are several correlations available to estimate the molecular weight as a function of boiling point, density and viscosity. In general, correlations that only require the boiling point are the least accurate and correlations that require values of boiling point, density and viscosity tend to be the most accurate. Viscosity is used as a parameter in these correlations because it correlates well with molecular type – which can further refine the molecular weight estimate. In most cases, we use correlations that require the boiling point and density of a given component. Two popular correlations are the Lee-Kesler [9, 10] correlation, Equation (1.8), and the Twu [11] correlation, Equations (1.9) to (1.12), respectively.

$$MW = -12272.6 + 9486.4(SG) + (8.3741 - 5.99175 \cdot SG) \, T_b \tag{1.8}$$

$$+ \left(1 - 0.77084 \cdot SG - 0.02058 \cdot SG^2\right) \cdot \left(0.7465 - \frac{222.466}{T_b}\right) \cdot \frac{10^7}{T_b}$$

$$+ \left(1 - 0.80882 \cdot SG - 0.02226 \cdot SG^2\right) \cdot \left(0.3228 - \frac{17.335}{T_b}\right) \cdot \frac{10^{12}}{T_b^3}$$

$$MW^0 = \frac{T_b}{5.8 - 0.0052 \, T_b} \tag{1.9}$$

$$SG^0 = 0.843593 - 0.128624 \, \alpha - 3.36159 \, \alpha^3 - 13749.5 \, \alpha^{12} \tag{1.10}$$

$$T_c^0 = T_b \left(0.533272 + 0.343838 \cdot 10^{-3} \cdot T_b + 2.52617 \cdot 10^{-7} \cdot T_b^2 \right. \tag{1.11}$$

$$\left. - 1.654881 \cdot 10^{-10} \cdot T_b^3 + 4.60773 \cdot 10^{-24} \cdot T_b^{-13}\right)^{-1}$$

$$\alpha = 1 - \frac{T_{\text{b}}}{T_{\text{c}}^0} \tag{1.12}$$

$$\ln(\text{MW}) = \ln\left(\text{MW}^0\right)\left[\frac{(1 + 2\,f_{\text{M}})}{(1 - 2\,f_{\text{M}})^2}\right] \tag{1.13}$$

$$f_{\text{M}} = \Delta\text{SG}_{\text{M}}\left[\chi + \left(-0.0175691 + \frac{0.143979}{T_{\text{bo.5}}}\right)\Delta\text{SG}_{\text{M}}\right] \tag{1.14}$$

$$\chi = \left|0.012342 - \frac{0.244515}{T_{\text{b}}^{0.5}}\right| \tag{1.15}$$

$$\Delta\text{SG}_{\text{M}} = \exp\left[5\left(\text{SG}^0 - \text{SG}\right)\right] - 1 \tag{1.16}$$

Riazi [4] lists several other correlations such as Cavett and Goosens for molecular weight, but they generally do not have significant advantage over the Lee-Kesler or Twu correlations. The Lee-Kesler correlation was developed by correlating light oil fractions (< 850 °F or 454 °C) from a variety of sources. As a result, the Lee-Kesler correlation tends to be less accurate for pseudocomponents with high boiling point temperatures. The Twu correlation includes a significant number of data points to account for heavier components. We recommend using the Twu correlation, especially for heavier feed types processed in the crude vacuum towers. The correlation is quite easy to change in most process modeling software. Figure 1.41 shows how to select the molecular weight correlation for a particular blend (shown in earlier workshops) in Aspen HYSYS.
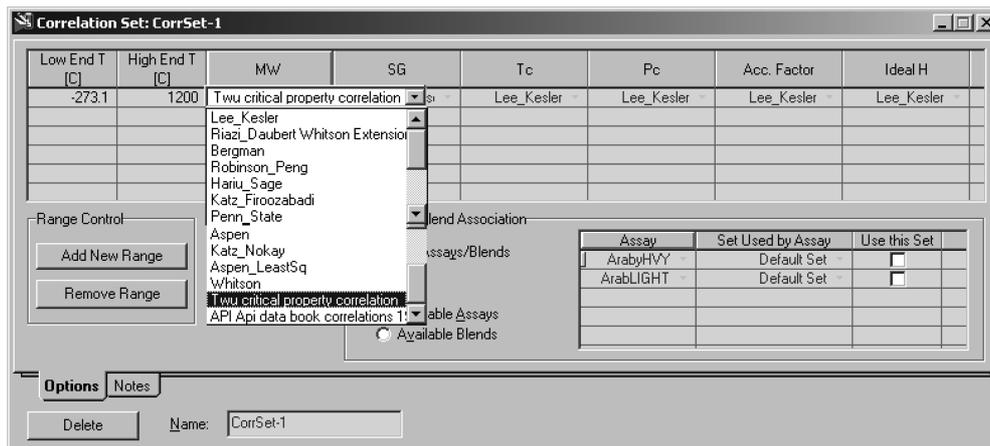

Figure 1.41 Modify molecular weight correlation in Aspen HYSYS.

1.8.3
Critical Properties

Many properties that are required for rigorous accounting of material and energy flows (Table 1.3) in process models are not well defined for pseudocomponents. Fortunately, researchers have found that these required properties correlate well with critical temperature (T_c), critical pressure (P_c) and acentric factor (ω) for different types of hydrocarbons from many sources. Therefore, when we use pseudocomponents of any kind, we must also estimate these critical properties. Just as with molecular weight, there are many critical property estimation methods available in the literature. These correlations differ on the basis of the parameters required and underlying data used to create the correlation. We note that as the components get heavier and boil at higher temperatures, the associated change in critical pressure tends to diminish. Hence, correlations for critical pressure tend to be logarithmic formulas. A modeling consequence is that particularly accurate measures of these critical pressures are not required for good modeling results. In addition, most refinery processes conditions do not approach the critical properties of these pseudocomponents.

Lee-Kesler [9, 10] and Twu [11] have also produced correlations for critical properties. In our work, we have used the Lee-Kesler correlations extensively. Equations (1.17) and (1.18) give the correlations for critical temperature (T_c) and critical pressure (P_c) using the Lee-Kesler correlations. We recommend using these correlations for all boiling-point ranges since the differences that arise from using other correlations are often minor. Figure 1.42 and Figure 1.43 show how we can change the correlation for each blend in Aspen HYSYS.

$$T_c = 189.8 + 450.6\,\text{SG} + \left(0.4244 + 0.1174\,\text{SG}\right) T_b \tag{1.17}$$
$$+ \left(0.1441 - 1.0069\,\text{SG}\right) \cdot 10^5 \big/ T_b$$

$$P_c = 5.689 - \frac{0.0566}{\text{SG}} - \left(0.43639 + \frac{4.1216}{\text{SG}} + \frac{0.21343}{\text{SG}^2}\right) \cdot 10^{-3}\, T_b \tag{1.18}$$
$$+ \left(0.47579 + \frac{1.182}{\text{SG}} + \frac{0.15302}{\text{SG}^2}\right) \cdot 10^{-6}\, T_b^2$$
$$- \left(2.4505 + \frac{9.9099}{\text{SG}^2}\right) \cdot 10^{-10}\, T_b^3$$

A related property is the acentric factor. The acentric factor accounts for the size and shape of various kinds of molecules. Simple molecules have an acentric factor close to 0, whereas large or complex hydrocarbon molecules may have values approaching 0.5 to 0.6[6]. The acentric factor is not measured, but defined as an explicit function of the ratio of vapor pressure at the normal boiling point to the measured or estimated critical pressure. We show the definition of the acentric factor in Equation (1.19).
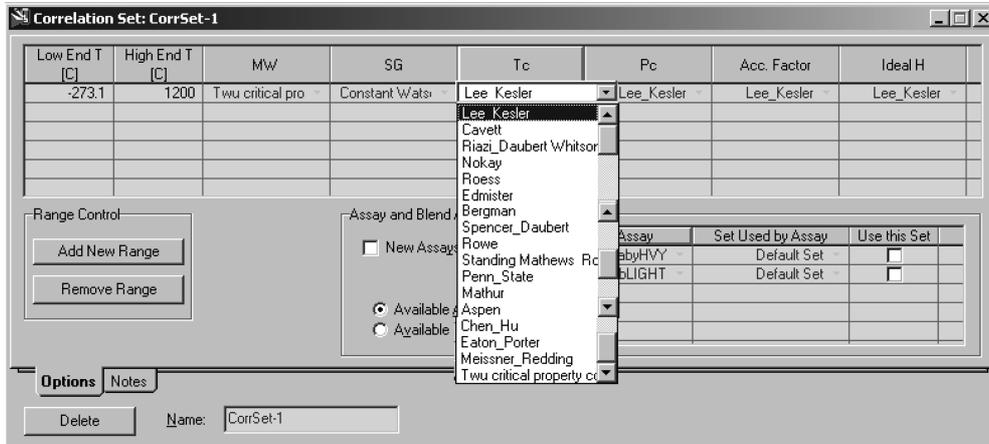
**Figure 1.42** Modify T_c correlation in Aspen HYSYS.
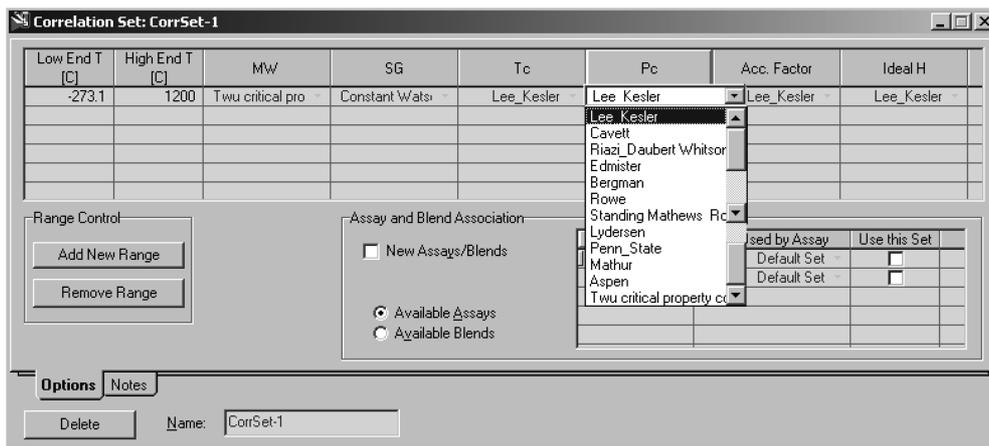
Figure 1.43 Modify P_c correlation in Aspen HYSYS.

$$\omega = -\log_{10}\left(P_r^{\text{VAP}}\right) - 1.0 \tag{1.19}$$

where P_r^{VAP} represents the reduced vapor pressure, that is, the pseudocomponent vapor pressure divided by its critical pressure, when the reduced temperature, T_r that is, the temperature divided by the critical temperature, is equal to 0.7.

Given the small range of values for the acentric factor, most correlations can provide useful results. The accuracy of the acentric correlation depends largely on the accuracy of the critical temperature and pressure correlations. However, even large relative errors do not result in significant deviation of derived properties such
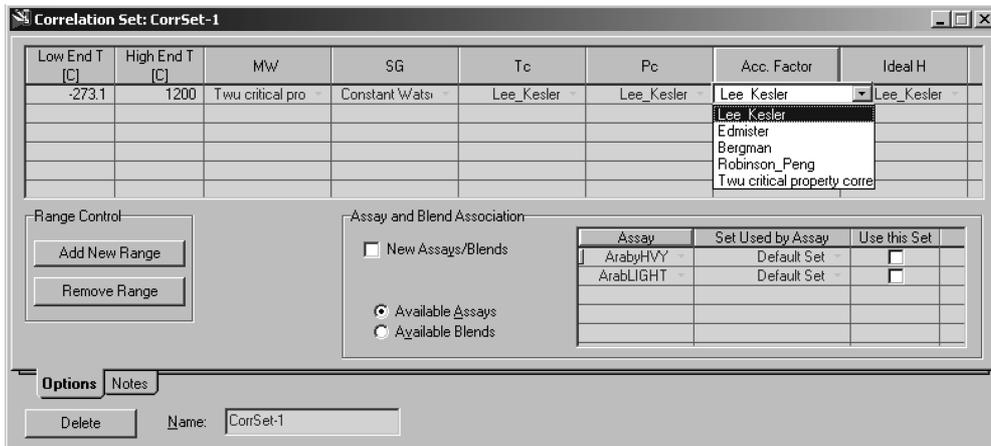
Figure 1.44 Modify acentric factor correlation in Aspen HYSYS.

as ideal gas heat capacity, etc. We again choose the Lee-Kesler [9, 10] correlation for the acentric factor. This correlation, given by Equation (1.16), relies on extensive vapor pressure data collected by Lee and Kesler for the critical temperature and pressure correlations. The correlation is technically limited to the reduced boiling point temperature (T_{br}) of less than 0.8, but has been successfully used at high T_{br} values. Figure 1.44 shows how we can modify the acentric factor estimation method for oil blends in Aspen HYSYS.

$$\omega = \frac{-\ln\left(P_C/1.01325\right) - 5.92714 + \dfrac{6.09648}{T_{br}} + 1.28862 \ln\left(T_{br}\right) - 0.169347 \, T_{br}^{6}}{15.2518 - \dfrac{15.6875}{T_{br}} - 13.4721 \ln\left(T_{br}\right) + 0.43577 \, T_{br}^{6}} \quad (1.20)$$

1.8.4
Liquid Density

The liquid density of hydrocarbons is essential for modeling purposes to convert molar and mass flows into volumetric flows. Many processes in the refinery operate on the basis of volumetric flow. In addition, the density of the products is an important constraint when marketing the refinery's products for sale. In the context of process modeling, liquid density is also a property parameter that must be correlated since many of the equation-of-state thermodynamic models cannot accurately predict liquid densities. Even when a given process modeling software uses an equation-of-state approach for refinery modeling, liquid density is often calculated independently to ensure accurate results. Figure 1.45 shows how Aspen HYSYS calculates liquid density independently even when we use an equation-of-state (in this case, Peng-Robinson method) as the thermodynamic model.
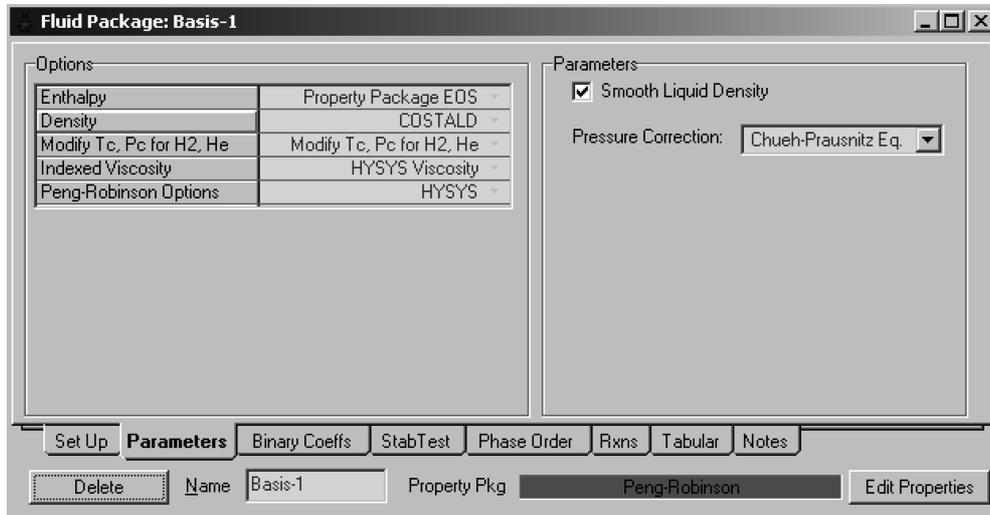
Figure 1.45 Options for Peng-Robinson equation-of-state in Aspen HYSYS.

There are several correlations available in the literature for liquid mass density or liquid molar volume as functions of various critical properties. It is possible to convert from the liquid mass density to liquid molar volume using the molecular weight of the component in question. This also means that errors in the molecular weight or critical properties predictions can introduce additional error in the liquid density or molar volume correlations. Popular correlations for the liquid density include Yen-Woods [12], Gunn-Yamada [13] and Lee-Kesler [9, 10]. An accurate correlation (when the reduced temperature is less than 1) of liquid density is the Spencer-Danner (modified Rackett) method [14] with COSTALD (Corresponding States Liquid Density) [15] correction for pressure. Equation (1.21) gives the standard Spencer-Danner equation. This equation actually predicts the molar volume at saturated liquid conditions. We can convert this molar volume to liquid density using the molecular weight.

$$V^{\text{SAT}} = \left(\frac{RT_C}{P_c} \right) Z_{\text{RA}}^n \quad \text{with } n = 1.0 + \left(1.0 - T_r \right)^{2/7} \tag{1.21}$$

$$Z_{\text{RA}} = 0.29056 - 0.08775\,\omega \tag{1.22}$$

Z_{RA} is a special parameter to account for the critical compressibility of the component. Tables of Z_{RA} for many pure components are part of the pure component databases in Aspen HYSYS. Z_{RA} for pseudocomponents may be estimated from Equation (1.22) as a function of the correlated acentric factor.

The liquid density from the Spencer-Danner equation is a function of temperature only. Refinery processing conditions can be severe enough where the liquid density is also a function of pressure. To correct the liquid density for high

pressure, we can introduce the COSTALD correction given by Equation (1.23). This equation requires the liquid density, ρ_{p^0}, at a certain reference pressure, P^0, obtained from Equation (1.22) and predicts the density, ρ_P, at an elevated pressure, P, as a function of two parameters, C and B.

$$\rho_P = \rho_{p^0} \left[1 - C \ln \left(\frac{B+P}{B+P^0} \right) \right]^{-1} \tag{1.23}$$

$$e = \exp \left(4.79594 + 0.250047\,\omega + 1.14188\,\omega^2 \right) \tag{1.24}$$

$$B = P_c \left[-1 - 9.0702 \left(1.0 - T_r \right)^{\frac{1}{3}} + 62.45326 \left(1.0 - T_r \right)^{\frac{2}{3}} \right.$$
$$\left. - 135.1102 \left(1.0 - T_r \right) + e \left(1.0 - T_r \right)^{\frac{4}{3}} \right] \tag{1.25}$$

$$C = 0.0861488 + 0.0344483\,\omega \tag{1.26}$$

The COSTALD correlation is quite accurate even at high reduced temperatures and pressures. Predicted liquid densities generally agree with measured values within 1–2% provided the errors in the critical property predictions are low. A potential problem can occur if the reduced temperature is greater than 1. There can be discontinuity from the Spencer-Danner equation in the density prediction which may cause some process models to fail. However, at a reduced temperature greater than 1, the equation of state becomes more accurate and can be used directly. Aspen HYSYS includes a smoothing approach (using the Chueh and Prausnitz correlation [16]) to ensure a smooth transition from the COSTALD densities to equation-of-state-based densities.

1.8.5
Ideal Gas Heat Capacity

The last property that is often directly correlated is the ideal gas heat capacity of pseudocomponents. The ideal gas heat capacity represents the vapor heat capacity of the pseudocomponent at a given standard condition. The standard conditions typically refer to 25 °C and 1 atm or 77 °F and 14.696 psia. It is well known the heat capacity of hydrocarbons can be modeled with a simple polynomial expression as a function of temperature. Lee and Kesler [9, 10] present a popular correlation where M is molecular weight, T in Kelvin, and K_w is Watson-factor. These parameters may be estimated from other correlations, including Lee-Kesler equation for MW in Section 1.8.2, Equation (1.8). The heat capacities of hydrocarbons do not vary significantly over a wide range of temperatures, so very accurate heat capacities are not necessary for good modeling results. We present this correlation in Equation (1.27).
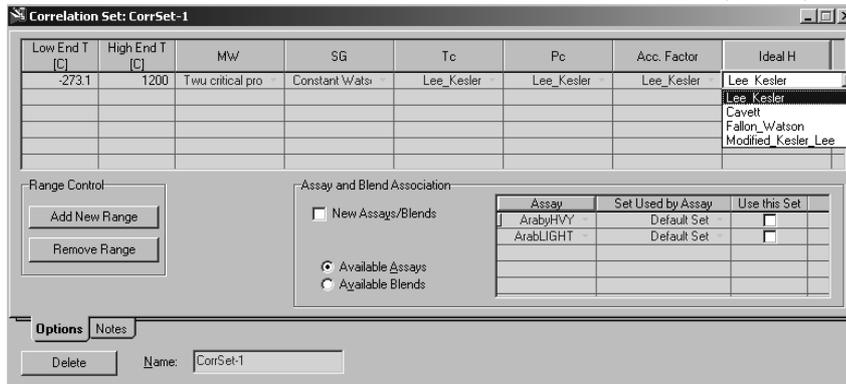
Figure 1.46 Modify the Ideal Gas Heat Capacity in Aspen HYSYS.

$$C_P^{IG} = MW \left[A_0 + A_1 \, T + A_2 \, T^2 - C \left(B_0 + B_1 \, T + B_2 \, T^2 \right) \right] \tag{1.27}$$

$$A_0 = -1.41779 + 0.11828 \, K_w \tag{1.28}$$

$$A_1 = -\left(6.99724 - 8.69326 \, K_w + 0.27715 \, K_w^2 \right) \cdot 10^{-4} \tag{1.29}$$

$$A_2 = -2.2582 \cdot 10^{-6} \tag{1.30}$$

$$B_0 = 1.09223 - 2.48245 \, \omega \tag{1.31}$$

$$B_1 = -\left(3.434 - 7.14 \, \omega \right) \cdot 10^{-3} \tag{1.32}$$

$$B_2 = -\left(7.2661 - 9.2561 \, \omega \right) \cdot 10^{-7} \tag{1.33}$$

$$C = \left[\frac{\left(12.8 - K_w \right) \cdot \left(10 - K_w \right)}{10 \, \omega} \right]^2 \tag{1.34}$$

1.8.6
Other Derived Physical Properties

Once we have obtained the boiling point, density or specific gravity, molecular weight and critical properties of a particular pseudocomponent, we can also generate estimates for other required properties for process simulation shown in Table 1.3. The accuracy of these predictions is largely a function of the accuracy of the molecular weight and critical property predictions. In addition, depending on the thermodynamic method chosen, we may not require any correlations for certain properties. For example, if we choose an equation-of-state approach, we do not require any additional correlations for the vapor pressure (P_{VAP}) or heat of vaporization (ΔH_{VAP}), since these values will be calculated directly by the equation

of state. We discuss such features of the equation of state in the following section. In this section, we present correlations for all required properties so that model developers are aware of the model limitations and additional data requirements when we do not use an equation of state for modeling process thermodynamics.

The liquid heat capacity of pseudocomponents involved refinery modeling is largely constant. Walas [6] notes that as the boiling point and density of the pseudo-component increases, the heat capacity of hydrocarbons tends to approach a value of 1.8–2.2 kJ/kg K near the normal boiling point. Consequently, rough estimates of heat liquid capacities do not affect model results significantly. There are two correlations available for liquid heat capacities of hydrocarbons that are in general use. Equation (1.35) is a correlation by Kesler and Lee [9, 10] and Equation (1.39) is a correlation recommended by API. Either correlation may be used with equal results. We generally do not encounter these temperature limits prescribed for both of these correlations. We also note that these correlations are weak functions of temperature. Process modeling software programs have a variety of models to estimate the liquid heat capacity, but these methods are only marginally better compared to the simple correlations given here.

When 145 K $< T < 0.8\ T_c$

$$C_P^L = a\left(b + c\ T\right) \tag{1.35}$$

$$a = 1.4651 + 0.2302\ K_w \tag{1.36}$$

$$b = 0.306469 - 0.16734\ SG \tag{1.37}$$

$$c = 0.001467 - 0.000551\ SG \tag{1.38}$$

When $T_r < 0.85$

$$C_P^L = A_1 + A_2\ T + A_3\ T^2 \tag{1.39}$$

$$A_1 = -4.90383 + \left(0.099319 + 0.104281\ SG\right) K_w \tag{1.40}$$
$$+ \left(\frac{4.81407 - 0.194833\ K_w}{SG}\right)$$

$$A_2 = \left(7.53624 + 6.214610\ K_w\right)\cdot\left(1.12172 - \frac{0.27634}{sG}\right)\cdot 10^{-4} \tag{1.41}$$

$$A_3 = -\left(1.35652 + 1.11863\ K_w\right)\cdot\left(2.9027 - \frac{0.70958}{SG}\right)\cdot 10^{-7} \tag{1.42}$$

Another property related to the heat capacity is the heat of vaporization of pseudocomponent as a liquid. The heat of vaporization represents the heat required to vaporize a given mass (or volume) of liquid into vapor. Like heat

capacities, there are several correlations to calculate the heat of vaporization in the literature. We present two popular correlations here. Equation (1.43) is the Riedel correlation [17] and Equation (1.44) is the Chen and Vettere [17] correlation. We note that both correlations rely on critical temperatures and pressure, and give the heat of vaporization at the normal boiling point. We can obtain the heat of vaporization at a different temperature by using the Watson relation [4] in Equation (1.45). Either of the correlations can provide very good results for hydrocarbons (< 2% average relative deviation, ARD). We recommend the use of either correlation if the process modeling software does not already include a correlation. In addition to these correlations, Aspen HYSYS offers a more advanced proprietary correlation using two Reference-state liquids.

$$\Delta H_{\text{NBP}}^{\text{VAP}} = 1.093 \ R \ T_{\text{c}} \ T_{\text{br}} \ \frac{\ln P_{\text{c}} - 1.013}{0.93 - T_{\text{br}}} \tag{1.43}$$

$$\Delta H_{\text{NBP}}^{\text{VAP}} = R \ T_{\text{c}} \ T_{\text{br}} \ \frac{3.978 \ T_{\text{br}} - 3.958 + 1.555 \ln P_{\text{c}}}{1.07 - T_{\text{br}}} \tag{1.44}$$

$$\Delta H^{\text{VAP}} = \Delta H_{\text{NBP}}^{\text{VAP}} \left(\frac{1 - T_{\text{r}}}{1 - T_{\text{br}}} \right)^{0.38} \tag{1.45}$$

The vapor pressure of pseudocomponents is also an important property when an equation-of-state approach is not used. All other approaches to process thermodynamics require some form of vapor-pressure correlation. The vapor pressure for pure hydrocarbons has been extensively tabulated in many component databases such as DIPPR (Design Institute for Physical Property Research, American Institute of Chemical Engineers) and significant libraries are available in modern process modeling software. Several correlations are available in the literature for the vapor pressure of pseudocomponents. It is important to recall that the vapor pressure and heat vaporization are related through the Clausius-Clapeyron [17] Equation (Equation (1.46)). This relationship imposes a constraint if we wish the model to be thermodynamically consistent. In general, most of the popular correlations for vapor pressure such as the Lee-Kesler [9, 10] agree well with heat of vaporization correlations and maintain thermodynamic consistency. We present the Lee-Kesler vapor pressure correlation in Equation (1.47).

$$\frac{\text{d} \ln P}{\text{d} T} = \frac{\Delta H_{\text{VAP}}}{R \ T^2} \tag{1.46}$$

$$\ln P_{\text{r}}^{\text{VAP}} = 5.92714 - \frac{6.096648}{T_{\text{r}}} - 1.28862 \ln T_{\text{r}} + 0.169347 \ T_{\text{r}}^6 \tag{1.47}$$
$$+ \ \omega \left(15.2518 - \frac{15.6875}{T_{\text{r}}} - 13.4721 \ln T_{\text{r}} + 0.43577 \ T_{\text{r}}^6 \right)$$

The Lee-Kesler correlation for vapor pressure is quite accurate for low to medium boiling pseudocomponents. For very light components, we recommend using pure component properties directly. In the case of heavy components, Ambrose [17] has presented an additional term for the Lee-Kesler correlation. In practice, however, the additional term is not necessary for refinery modeling purposes.

1.9
Process Thermodynamics

After we have fully characterized the pseudocomponent and any true components in the process model, we must choose a thermodynamic model. The thermodynamic model here refers to a framework that allows us to describe whether a particular mixture of components forms one phase or two phases, the distribution of components within these phases and material and energy flows of these phases given a set of process conditions. Process thermodynamics also set material and energy transfer limits on various fractionation and reaction units in the model and in the actual plant itself.

Modern refineries deal with a multitude of complex systems that may require different thermodynamic models for each refinery plant and its associated process model. For example, we cannot model the sour gas units that deal with acid gases and water with the same thermodynamic model that we use for the crude fractionation system. In fact, reasonable thermodynamic models form the heart of any process model. Chen et al. [7] have documented the variety of thermodynamic models available for frequently encountered chemical and physical systems. Agarwal et. al [18] present a detailed account about the pitfalls of choosing a poor thermodynamic system for process models and the undesired consequences of using these poor models to modify plant operations. Process model developers and users must be aware of the underlying thermodynamics and its limitations.

Given that the field of thermodynamic models is vast, we choose to focus on thermodynamic models that deal with hydrocarbon-hydrocarbon interactions only, which can model many units in the refinery quite accurately. The only complication (aside from the choice of an appropriate thermodynamic model) is the presence of large amounts of water in the form of steam in various fractionation and reaction units. In most cases, we can simply deal with the hydrocarbon and water phases as immiscible. This is known as the "free-water" approach. Kaes [1] discusses this approach extensively and it is a common approach in many process simulators. Some software may include a "dirty-water" approach. This approach uses correlations to model the solubility of water in the hydrocarbon and the solubility of light acid gases in water. For the purposes of refinery reaction and fractionation modeling in this text, both approaches have negligible effects on the overall process model. We give the general statement of vapor-liquid equilibrium for any thermodynamic model in Equation (1.48):

$$\gamma_i \; \varphi_i^{V} \; P = x_i \; \varphi_i^{L} \; P \tag{1.48}$$

where γ_i refers to vapor-phase molar composition of component i, φ_i^V refers to the vapor-phase fugacity coefficient of component i, P is overall pressure, x_i is the liquid-phase molar composition of component i and φ_i^L refers to the liquid-phase fugacity coefficient of component i. For refinery fractionation modeling, several simplifications are possible. Each one of these simplifications represents a different thermodynamic approach. We list major approaches, required pseudo-component properties and our recommendation for use in Table 1.4. We discuss each of these approaches and their requirements in subsequent sections.

Table 1.4 Comparison of various thermodynamic approaches.

Approach	Required Physical Properties	Recommended
Simple	Molecular Weight (MW) Ideal Gas Heat Capacity (CP_{IG}) Vapor Pressure (P_{VAP}) Heat of Vaporization (ΔH_{VAP}) Liquid Heat Capacity (CP_{LIQ}) Liquid Density (ρ_L)	No
Mixed or activity coefficient	Molecular Weight (MW) Ideal Gas Heat Capacity (CP_{IG}) Vapor Pressure (P_{VAP}) Heat of Vaporization (ΔH_{VAP}) Liquid Heat Capacity (CP_{LIQ}) Liquid Density (ρ_L) Solubility Parameter (δ)	Yes, however, best with heavy components that the EOS approach cannot deal with
Equation of state	Molecular Weight (MW) Critical Temperature (T_c) Critical Pressure (P_c) Acentric Factor (ω) Ideal gas Heat Capacity (CP_{IG}) Liquid Density (ρ_L) Interaction Parameter (k_{ij})	Yes, with adequate corrections of liquid density

1.9.1
Thermodynamic Models

The simple approach is the most basic and least rigorous thermodynamic approach. In the simple approach or the Raoult's law, we assume that both the vapor and liquid phases are ideal. In this case, the general statement of equilibrium (Equation (1.48)) may be written as Equation (1.49), where γ_i is the vapor-phase mole composition of component i, P is the pressure, x_i is the liquid-phase mole composition and $P^{SAT}(T)$ is the vapor pressure of component i as a function of temperature only. These properties are routinely available for pure components and we have extensively discussed how to obtain the required properties from pseudocomponents.

$$\gamma_i \, P = x_i \, P^{SAT}(T) \tag{1.49}$$

A variation of this equation is to re-arrange the equation to obtain the equilibrium distribution ratio, γ_i/x_i as shown in Equation (1.50). This distribution ratio is also known as the *K*-value for component i. Numerous correlations for *K*-values exist for a variety of pure components and pseudocomponents. The Braun-K10 (BK-10) correlation is a popular correlation of this type [6].

$$K_i = \frac{\gamma_i}{x_i} = \frac{P^{SAT}(T)}{P} = f(T) \tag{1.50}$$

Once we obtain a *K*-value at a given temperature and pressure, we can perform mass and energy balances include isothermal, isobaric and isenthalpic flashes. We can also use the ideal gas heat capacity of the vapor phase, heat of vaporization and heat of capacity of the liquid to represent the enthalpies of relevant vapor and liquid streams.

Most process simulators include these types of correlations but they are largely of historical interest or used to maintain compatibility with old models. We do not recommend using simple methods, since they cannot adequately quantify the transition from vapor to liquid phases beyond the original correlation. In addition, these correlations tend to be thermodynamically poor (do not consider any interactions between components and thermodynamically inconsistent at higher pressures) and we cannot integrate models using these correlations into new models that use an equation of state or activity coefficient approach without significant efforts.

1.9.2
Mixed or Activity-Coefficient Approach

The mixed or activity-coefficient approach uses the concept of activity coefficients to separate out the effects of non-ideality because of component interactions and the effect of pressure. For the activity-coefficient approach, we can rewrite the general equilibrium statement as:

$$\gamma_i \, \varphi_i^V \, P = x_i \, \gamma_i \, \varphi_i^{SAT} \, P^{SAT}(T) \, PF_i \tag{1.51}$$

$$PF_i = \exp\left(\int_{P^{SAT}}^{P} \frac{V_i(T,\pi)}{R\,T} \, d\pi \right) \tag{1.52}$$

where γ_i is vapor mole composition of component i, φ_i^V is the vapor-phase fugacity coefficient for component i, P is the system pressure, x_i is the liquid mole composition of component i, φ_i^{SAT} is the fugacity coefficient for vapor pressure of component i, $P^{SAT}(T)$ is the vapor pressure of component i and PF_i is the Poynting

factor for component i at pressure P, V_i is the molar volume of component i as a function of temperature, T and pressure, π (integrated from P^{SAT} to P). The PF_i factor is generally close to a value of 1 unless the system pressure is very high [17]. We can rewrite the equilibrium relationship in the form of *K*-values as Equation (1.53).

$$K_i = \frac{\gamma_i}{x_i} = \frac{\gamma_i \, \varphi_i^{SAT} \, P^{SAT}(T)}{\varphi_i^{V} \, P} \qquad (1.53)$$

We can now use the Redlich-Kwong equation of state [6] and a liquid-phase correlation (or an equation of state) to obtain expressions for φ_i^{V} and φ_i^{SAT} as functions of temperature, pressure and component critical properties. This is the approach taken by the very popular Chao-Seader [6] and Grayson-Streed [6] methods. The only factor that remains undefined is the liquid activity coefficient. The Chao-Seader and Grayson-Streed methods use the regular solution theory to obtain an expression for γ_i as follows:

$$\ln \gamma_i = \frac{V_i}{R \, T} \left(\delta_i - \overline{\delta} \right) \qquad (1.54)$$

$$\overline{\delta} = \frac{\sum x_i \, V_i \, \delta_i}{\sum x_i \, V_i} \qquad (1.55)$$

where V_i is the liquid molar volume of component i and δ_i is the solubility parameter for component i. Molar volumes for pure components are readily available and we discussed several methods to estimate molar volumes for pseudocomponents in Section 1.8.4. We can obtain the solubility parameter for pseudocomponents using Equation (1.56) where ΔH_{VAP} is the heat of vaporization, R is the universal gas constant and T is system temperature. We have discussed how to calculate the heat of vaporization for pseudocomponents in Section 1.8.6.

$$\delta_i = \left(\frac{\Delta H_{VAP} - R \, T}{V_i} \right)^{0.5} \qquad (1.56)$$

We can now use the *K*-value expression to calculate various equilibrium properties and perform typical flash calculations. As with the simple thermodynamic approach, we can use the heat capacities, and heats of vaporization to obtain enthalpy balances for vapor and liquid streams. In addition, since we account for vapor- and liquid-phase non-ideality due to component interactions, and temperature and pressure effects, we can also apply standard thermodynamic relationships to compute excess properties for enthalpies, etc. The excess properties account for deviations from an ideal mixing behavior and the resulting deviations in equilibrium behavior.

Using the activity-coefficient approach in the form of the Chao-Seader or Grayson-Streed method for refinery modeling is a significant improvement over the simple approach. The activity-coefficient approach accounts for vapor- and liquid-phase non-idealities accurately in both the equilibrium and enthalpy calculations. In addition, this approach is easy to integrate with other types of activity-coefficient models that we may use in refinery models (especially for sour water systems). We prefer to use activity-coefficient models when dealing with heavy components that occur especially in vacuum distillation systems. A key shortcoming of this approach is that light components may require fictitious solubility parameters fitted to certain data sets and performance of this approach degrades quickly near the vicinity of the critical point. In general, however, this method is a reasonable thermodynamic model for real and pseudo components that we find in refinery reaction and fractionation systems.

1.9.3
Equation-of-State Approach

The most rigorous approach is the equation of state (EOS) approach. When we use an EOS, both vapor and liquid phases uses the same model. We do not modify the general equilibrium statement from Equation (1.48) because we can calculate the fugacity coefficients directly after we choose a particular EOS.

There are many types of EOS with a wide range of complexity. The Redlich-Kwong (RK) EOS is a popular EOS that relies only on critical temperatures and critical pressures of all components to compute equilibrium properties for both liquid and vapor phases. However, the RK EOS does not represent liquid phases accurately and is not widely used, except as a method to compute vapor fugacity coefficients in activity-coefficient approaches. On the other hand, the Benedict-Webb-Rubin-Starling (BWRS) EOS [6] has up to sixteen constants specific for a given component. This EOS is quite complex and is generally not used to predict properties of mixture with more than few components.

For the purposes of refinery fractionation and reaction modeling, the most useful EOS models derive from either the Peng-Robinson (PR) EOS [6] or the Soave-Redlich-Kwong (SRK) EOS [6]. Both the PR and SRK EOS are examples of cubic equations of state. Cubic EOS'es are quick and easy to use for modeling work and provide a good balance between thermodynamic robustness and prediction accuracy. In our work, we have used the PR EOS with good results throughout many reaction and fractionation processes in refineries. There are more advanced EOS models that can be used in the context of refinery modeling, but we limit the scope of our discussion to the PR EOS.

We give the basic form of the PR EOS in Equation (1.63). The PR-EOS requires three main properties: critical temperature, critical pressure and the acentric factor.

$$a_i = 0.45724 \; R^2 \; \frac{T_{c_i}^2}{P_{c_i}} \tag{1.57}$$

$$b_i = 0.07780 \ R \ \frac{T_{c_i}}{P_{c_i}} \tag{1.58}$$

$$a_i = \left[1 + \left(0.37464 + 1.5426 \ \omega_i - 0.26992 \ \omega_i^2 \right) \left(1 - T_{r_i}^{0.5} \right) \right]^2 \tag{1.59}$$

$$aa_{MIX} = \sum \sum x_i \ x_j \ (aa)_{ij} \tag{1.60}$$

$$b_{MIX} = \sum x_i \ b_i \tag{1.61}$$

$$aa_{ij} = \sqrt{aa_{ii} \ aa_{jj}} \ \left(1 - k_{ij} \right) \tag{1.62}$$

$$P = \frac{R \ T}{V_{MIX} - b_{MIX}} - \frac{aa_{MIX}}{V_{MIX}^2 + 2 \ b_{MIX} \ V_{MIX} + b_{MIX}^2} \tag{1.63}$$

where V_{MIX} is the molar volume of the mixture and k_{ij} is an interaction parameters for each i and j pair of components. The critical properties and interaction parameters for a large number of pure components are available within most process modeling software tools. We discussed how to obtain the critical properties of pseudocomponents in Section 1.8.3. In general, we can set the interaction parameters for pseudocomponents to 0 without significantly changing model results. Riazi [4] discusses several correlations to estimate the interaction parameters as functions of critical volumes of the components.

The EOS approach is robust and can generate the vapor pressure, heat of vaporization, liquid density and liquid heat capacity using standard thermodynamic relationships and basic information such as critical properties and ideal gas heat capacities for all components. We refer the reader to the excellent text by Poling et al. [17] where there are detailed formulas for estimating all these derived properties from the EOS directly. In general, the PR EOS makes good predictions of equilibrium distributions for light- and medium-boiling components. In addition, we ensure the thermodynamic consistency by design since we use the same model for the vapor and liquid phases. The PR-EOS also generates mostly acceptable predictions for vapor and liquid enthalpy and displays good behavior near the critical point.

A key shortcoming in the EOS approach (specifically PR) is that predictions of liquid density are quite poor and not sufficiently accurate for process modeling purposes. The most popular method to deal with this problem is to ignore liquid density prediction from the EOS and use COSTALD method described in Section 1.8.4 to provide accurate density predictions. With similar reasoning, some process modeling software programs replace the enthalpy methods of EOS with Lee-Kesler correlations for heat capacity and enthalpy. However, this is not entirely necessary given the inaccuracies in the pseudocomponent physical properties predictions themselves. Finally, the presence of very light components such

as hydrogen and helium can sometimes provide spurious results. Aspen HYSYS includes several modifications (shown in Figure 1.45) for light components to prevent undesired behavior of light components. In general, we recommend using the EOS approach when developing refinery reaction and fractionation process models.

1.10
Miscellaneous Physical Properties for Refinery Modeling

In addition thermophysical properties required for modeling purposes, a complete model must also make predictions regarding several fuel properties routinely measured at the refinery. Typically these fuel or product properties include measurements such as flash point, freeze point, cloud point and paraffin-naphthene-aromatic (PNA) content. These properties not only serve as indicators of product quality and distribution, but may also be limited by government or internal refinery regulations. We can often justify the use of process modeling in the refinery by making sure that models also include predictions of these useful fuel properties. We will briefly discuss two approaches in this area and give concrete examples with flash point, freeze point and PNA content. We choose these particular properties because they display characteristics common to many types of fuel property correlation methods. We refer the reader to API standards [35] and Riazi [4] for more detailed expositions on various types of correlations for fuel properties not discussed in this section.

1.10.1
Two Approaches for Estimating Fuel Properties

Fuel or product properties can be a complex function of feed composition, process conditions and analysis method. It is generally not possible to take into account all of these variables when estimating fuel properties. The simplest approach is to correlate the relevant fuel property against modeled or measured bulk properties. For example, the flash maybe correlated with the 10% point of the ASTM D-86 curve. We can obtain the required distillation curve from the pseudocomponent stream composition. The software accomplishes this task by arranging pseudocomponents in ascending order of boiling point and creating a running cumulative sum of the liquid fractions of these pseudocomponents. This process results in the TBP curve of a given stream. Most software programs (including Aspen HYSYS) include methods to automatically convert this TBP curve into ASTM D-86 or D-1160 curves. Once we obtain this distillation curve, we can use several correlations to estimate the flash point, freeze point, etc. This method is simple to use and adaptable to any process simulator. However, this method relies on the availability of good correlations. It is important to remember that such correlations may not be valid or accurate for refineries that process frequently changing feedstocks. A second approach is to use indexes based on pseudocom-

ponent compositions. In an *index-based approach*, we represent each fuel property using the following equation:

$$\text{PROP}_{\text{MIX}} = \sum_{i=0}^{N} \text{PROP}_i \, w_i \qquad (1.64)$$

where PROP_{MIX} represents a given fuel property, PROP_i represents the property index for pseudocomponent i, w_i corresponds to the liquid, molar or weight fraction and N is the total number of pseudocomponents. Process modeling software tools and the literature have used this approach to quantify fuel properties such as octane numbers. An important advantage of this approach is that the property prediction can be tuned to a particular plant by modifying the value of PROP_i. This allows the model user to track plant performance accurately. This method is also very useful when attempting to correlate the flash point of various blends of fuels. However, this approach is generally not portable across various process modeling software programs and requires a large initial data set to regress starting values for PROP_i. In addition, there is a danger of over-fitting these values to match the plant performance. Overfitting the property indexes renders the model less useful for predictive purposes. In our work, we have used both approaches with equal success. However, for simplicity, we recommend the first approach; especially in light of the fact that large sets of data may not be available for determining initial PROP_i values.

1.10.2
Flash Point

The *flash point* of a fuel typically refers the temperature at which the fuel can ignite in the presence of an ignition source and sufficient air. A low flash point is an important consideration for gasoline engines since "sparking" or igniting the gasoline fuel is critical to optimum engine performance. In contrast, engines that use diesel and jet fuels do not rely on ignition (but on compression) and require fuels with a high flash point. The API [35] has correlated numerous data for a variety of fuels and found that the open- and closed-cup flash points (alternative measurement methods) linearly correlate well with the 10% ASTM D-86 distillation temperature. The flash point correlation is given by:

$$\text{FP} = A \left(\text{D86}_{10\%} \right) + B \qquad (1.65)$$

where FP is the flash point measured in °F, $\text{D86}_{10\%}$ refers to the 10% distillation temperature measured in °F. A and B are specific constants for various feed types. Typical values of A and B are 0.68–0.70 and 110–120, respectively. We recommend performing a simple linear regression to tune existing measurements into this correlation. API notes that this correlation may be improved using the 5% distillation temperature instead of the 10% distillation temperature. Deviations of 5–7 °F are within the tolerance of this correlation.

1.10.3
Freeze Point

The *freeze point* refers to the temperature at which solid crystals start to appear as a given fuel sample is being cooled. The freeze point dictates how a given fuel may be sold and if additives or blendings are required to ensure that the fuel does not clog engines at low ambient temperatures. A related concept is the cloud point. The cloud point is the temperature at which the sample takes a cloudy appearance. This is due to the presence of paraffins which solidify at a higher temperature than other components. The freeze point and cloud point do not correlate well with each without considering the paraffin content of the stream. The API [35] has correlated freeze point as follows:

$$\text{FRP} = A\,(\text{SG}) + B\,(K_w) + C\,(\text{MeABP}) + D \tag{1.66}$$

where FRP is the freeze point in °F, SG is the specific gravity, K_w is the Watson *K*-Factor and MeABP refers to the mean-average boiling point. *A, B, C* and *D* refer to specific constants for a given fuel composition. Typical values for *A, B, C* and *D* are 1830, 122.5, –0.135 and –2391.0, respectively. We can also fix the value of K_w to a constant (roughly 12) for narrowly distributed petroleum cuts. We can calculate the value of MeABP using the spreadsheet procedure described in Section 1.3. It is important to compare this correlation to that for the flash point. This correlation uses more bulk measurements (SG and K_w) to capture the effect of feed composition on the freeze point.

1.10.4
PNA Composition

The last sets of correlations we will address are composition correlations. These correlations identify chemical composition in terms of *total paraffin, naphthene and aromatic (PNA) content* of a particular feed based on key bulk measurements. These correlations are useful in two respects. First, we use these correlations to screen feeds to different refinery reaction units. For example, we may wish to send a more paraffinic feed to a reforming process when we want to increase the yield of aromatic components from the refinery. Secondly, these types of correlations form the basis of more detailed lumping for kinetic models that we will discuss at great length in subsequent chapters of this book. We will use these types of correlations to build extensive component lists that we can use to model refinery reaction processes.

Compositional information is quite useful to the refiner and many correlations are available in the literature that attempt to correlate PNA content to various bulk measurements. In general, these correlations rely on density or specific gravity, molecular weight, distillation curve and one or more viscosity measurements. The n-d-M (refractive index, density, and molecular weight) [4], API/Riazi-Daubert [35, 4], and TOTAL [19] correlations are just a few of the correlations available.

The Riazi-Daubert correlation relies on the most directly observed information and we expect it to show the smallest deviation from measured values. The other correlations require parameters (aniline point, etc.) that may not be routinely measured for all feeds. The Riazi-Daubert correlation takes the form:

$$\%X_P \text{ or } \%X_N \text{ or } \%X_A = A + B \cdot R_i + C \cdot \text{VGC}' \tag{1.67}$$

where $\%X$ represents the percent molar or volumetric composition of paraffins, naphthenes or aromatics (based on subscript chosen); R_i is the refractive index and VGC$'$ is the viscosity gravity constant or viscosity gravity factor. Coefficients A, B and C take on different values based on whether an aromatic, naphthene or paraffin is chosen as the subscript. This correlation can provide reasonably accurate results when we know the values of key input parameters with high accuracy. Overall, this method indicates a 6–7% absolute average deviation (AAD) from known measurement test cases.

We have extended the correlation by Riazi [4] to include the specific gravity, refractive index and the stream viscosity. Our updated correlation is given by:

$$\%X_P \text{ or } \%X_A = A + B \cdot \text{SG} + C \cdot R_i + D \cdot \text{VGC}' \tag{1.68}$$

$$\%X_N = 1 - \left(X_P + X_A\right) \tag{1.69}$$

where $\%X$ represents the percent molar or volumetric composition of paraffins, naphthenes or aromatics (based on subscript chosen); SG is the specific gravity, R_i is the refractive index and VGC$'$ is the viscosity gravity constant or viscosity gravity factor. In addition, the constants A to D are given for paraffins and naphthenes and for each fuel type. We show our updated t constants in Table 1.5 and Table 1.6. We also group the constants in this updated correlation by boiling-point ranges (Light Naphtha, etc.). This correlation reproduces plant data with 3–4% AAD, which is a significant improvement over the Riazi-Daubert correlation.

Table 1.5 Coefficients for paraffin content in petroleum fractions.

Boiling-point range	Paraffin (vol.%)				
	A	**B**	**C**	**D**	**AAD**
Light Naphtha	311.146	–771.335	230.841	66.462	2.63
Heavy Naphtha	364.311	–829.319	278.982	15.137	4.96
Kerosene	543.314	–1560.493	486.345	257.665	3.68
Diesel	274.530	–712.356	367.453	–14.736	4.01
VGO	237.773	–550.796	206.779	80.058	3.41

Table 1.6 Coefficients for aromatic content in petroleum fractions.

Boiling-point range	Aromatic (vol.%)				
	A	**B**	**C**	**D**	**AAD**
Light Naphtha	−713.659	−32.391	693.799	1.822	0.51
Heavy Naphtha	118.612	−447.589	66.894	185.216	3.08
Kerosene	400.103	−1500.360	313.252	515.396	1.96
Diesel	228.590	−686.828	12.262	372.209	4.27
VGO	−159.751	380.894	−150.907	11.439	2.70

We show how the grouping constants by boiling-point ranges can be useful when creating kinetic lumping procedures for the FCC in Chapter 4 of this text.

1.11
Conclusions

This chapter discusses several key modeling steps regarding thermophysical properties of crude oil and petroleum fractions. The basic process for developing a set of pseudocomponents for modeling refinery fractionation systems is as follows:

1. The feed to the fractionation system is often poorly defined in terms of actual components. We may only have an assay and associated bulk property measurements (such as density). We use the techniques discussed in Sections 1.1–1.3 to produce a complete TBP distillation curve and a density or specific gravity distribution.
2. Once we obtain the TBP and density curve, we can cut the components into a number of pseudocomponents. Each of these pseudocomponents has at least a TBP and density, by definition. The number of pseudocomponents for each cut point range can vary depending on the product range of the fractionation system. We have suggested the number of pseudocomponents for a few product ranges in Table 1.2. Subsequent chapters of this text include more information for specific fractionation systems.
3. After obtaining the pseudocomponents, we decide how to model key physical properties (Section 1.8) for these components. Process modeling software often includes a large variety of correlations and estimation methods. However, for almost all cases, the Lee-Kesler correlations for critical properties and ideal gas heat capacities are sufficient. We have used the extended Twu correlation for molecular weight in our work. After obtaining the critical properties and molecular weight for a given pseudocomponent, we may estimateall other required properties (heat capacities, etc.) with correlations given by Riazi.

4. We also select a thermodynamic system to model vapor-liquid equilibrium for these pseudocomponents. For crude fractionation columns, an euqation-of-state (EOS) approach yields good results. However, an EOS approach does not predict liquid densities accurately and tends to give poor equilibrium predictions of heavy pseudocomponents. We can improve the EOS density predictions with more accurate density correlations such as COSTALD. If the feed and products contain significant amounts of heavy products, it may be better to rely on empirical thermodynamic models such as Grayson-Streed or BK-10.

5. Lastly, we must make sure to use the product pseudocomponent information to verify measured product properties. In this chapter, we have discussed the flash point, freeze point and chemical composition properties of the products. The reader may find additional correlations for other fuel properties from the API handbook [2] and work by Riazi [4].

While this chapter has focused extensively on the requirements for modeling fractionation systems, we can use the same techniques in the context of modeling refinery reaction process as well. We illustrate this process in Chapters 4 through 6 of this text. It is possible to obtain good predictive results for fractionation systems provided that we make reasonable choices for the thermodynamic models and physical properties of the pseudocomponents involved.

1.12
Nomenclature

$A,\ B,\ \alpha,\ \beta$	Fitting parameters for cumulative beta distribution
C_p^{IG}	Ideal gas heat capacity, J/mol K
C_p^{L}	Liquid heat capacity, J/mol K
δ	Solubility parameter, $(J/cc)^{0.5}$
$\overline{\delta}$	Mean weighted solution solubility parameter, $(J/cc)^{0.5}$
$D86_{10\%}$	10% ASTM D-86 distillation point, °F
FP	Flash point, °F
FRP	Freeze point, °F
γ	Activity coefficient, unitless
ΔH_{VAP}	Heat of vaporization, J/mol
ΔH_{VAP}^{NBP}	Heat of vaporization at normal boiling point temperature, J/mol
K_i	K-value, ratio of γ_i/x_i, unitless
K_w	Watson K-Factor, unitless
K_{avg}	Watson K-Factor, unitless

k_{ij}	Interaction parameter for component i and component j in PR-EOS, unitless
MeABP	Mean average boiling point temperature, K
MW	Molecular weight, g/mol
P	Pressure, bar
P_c	Critical Pressure, bar
P_r	Reduced Pressure = P/P_c, unitless
P^{SAT}	Saturation or vapor pressure, bar
PF_i	Poynting correction factor, unitless
$PROP_{MIX}$	Mixture of indexed fuel properties
$PROP_i$	Fuel property index for a given component
φ_i^V	Vapor phase fugacity coefficient for component i
φ_i^{SAT}	Liquid phase fugacity coefficient corrected to saturation pressure for component i
φ_i^L	Liquid phase fugacity coefficient for component i
R	Universal gas constant, 8.315 J/mol K
T	Temperature, K
T_c	Critical Temperature, K
T_r	Reduced Temperature = T/T_c, unitless
T_b	Boiling point temperature, K
T_{br}	Reduced boiling point temperature = T_b/T_c, unitless
ρ_L	Liquid density, g/cc
ρ_P	Liquid density at pressure P, g/cc
ρ_P^0	Liquid density at reference pressure P^0, g/cc
R_i	Refractive index, unitless
SG	Specific Gravity, unitless
V^{SAT}	Molar volume of saturated liquid, cc/mol
V_i	Molar volume of component i as a function of temperature and pressure, cc/mol
VGC′	Viscosity Gravity Constant or Viscosity Gravity Factor, unitless
w_i	Weighting factor for property index mixing
$\%X_P$	Molar or volumetric composition of paraffins
$\%X_N$	Molar or volumetric composition of naphthenes
$\%X_A$	Molar or volumetric composition of aromatics
x_i	Liquid phase composition of component i
y_i	Vapor phase composition of component i
Z_{RA}	Rackett parameter, unitless
ω	Acentric factor, unitless

1.13
References

1 Kaes, G. L. *Refinery Process Modeling A Practical Guide to Steady State Modeling of Petroleum Processes*; The Athens Printing Company: Athens, GA, 2000.

2 Daubert, T. E.; Danner, R. P. *API Technical Data Book – Petroleum Refining*, 6th ed., American Petroleum Institute: Washington D. C., 1997.

3 Bollas, G. M.; Vasalos, I. A.; Lappas, A. A.; Iatridis, D. K.; Tsioni, G. K. Bulk Molecular Characterization Approach for the Simulation of FCC Feedstocks, *Ind. Eng. Chem. Res.* 2004, 43, 3270.

4 Riazi, M. R. *Characterization and Properties of Petroleum Fractions*; 1st ed., American Society for Testing and Materials: West Conshohocken, PA, 2005.

5 Sanchez, S.; Ancheyta, J.; McCaffrey, W. C.; Comparison of Probability Distribution Functions for Fitting Distillation Curves of Petroleum, *Energy & Fuels* 2007, 21, 2955.

6 Walas, S. M. *Phase Equilibria in Chemical Engineering*; Butterworth-Heinemann: Burlington, MA, 1985.

7 Chen, C. C.; Mathias, P. M. Applied Thermodynamics for Process Modeling, *AIChE J.* 2002, 48, 194.

8 de Hemptinne, J. C.; Behar, E. Thermodynamic Modeling of Petroleum Fluids, *Oil Gas Sci. Tech.* 2006, 61, 303.

9 Lee, B. I; Kesler, M. G. "A Generalized Thermodynamic Correlation Based on Three-Parameter Corresponding States." AIChE J. 1975, 21, 510.

10 Kesler, M. G.; Lee, B. I. "Improve Prediction of Enthalpy of Fractions." Hydrocarbon Processing. 1976, 55, 153.

11 Twu, C. H. "An Internally Consistent Correlation for Predicting the Critical Properties and Molecular Weights of Petroleum and Coal-Tar Liquids." Fluid Phase Equilibria. 1984, 16, 137.

12 Rackett, H. G., "Equation of State for Saturated Liquids", Journal of Chemical and Engineering Data. 1970, 15, 514.

13 Yamada, T. G. "Saturated Liquid Molar Volume: the Rackett Equation", Journal of Chemical Engineering Data. 1973, 18, 234.

14 Spencer, C. F. and Danner, R. P. "Improved Equation for the Prediction of Saturated Liquid Density" Journal of Chemical and Engineering Data. 1972, 2, 236.

15 Thomson, G. H., Brobst, K. R. and Hankinson, R. W. "An Improved Correlation for Densities of Compressed Liquids and Liquid Mixtures" AIChE J. 1982, 28, 671.

16 Cheuh, P. L. and Prausnitz, J. M. "A Generalized Correlation for the Compressibilities of Normal Liquids" AIChE J. 1969, 15, 471.

17 Poling, B. E.; Prausnitz, J. M; O'Connell, J. P. *Properties of Gas and Liquids*. 5th ed., McGraw-Hill, New York, 2000.

18 Agarwal, R.; Li, Y. K; Santollani, O.; Satyro, M. A.; Vieler, A. "Uncovering the realities of simulation" Chemical Engineering Progress. May, 2001. 42.

19 Sadeghbeigi, R. *Fluid Catalytic Cracking Handbook: Design, Operation and Troubleshooting of FCC Facilities.* **2000.** Gulf Publishing Company. Houston, TX.